https://doi.org/10.1016/j.ccr.2017.08.007

Manuscript Details

Manuscript number	CCR_2017_236
Title	Energy materials based on metal Schiff base complexes
Article type	Review Article

Abstract

Metal Schiff base complexes represent a class of compounds that have become a field of immense interest because of their intriguing chemical and physical properties, and their wide-ranging applications in a number of scientific areas. The presence of transition metal elements with a polydentate Schiff base ligand to form metal complexes offers a good platform for combining the chemical, electronic, magnetic, optical and redox properties of metal complexes with those of the organic materials. Metal Schiff base complexes can be incorporated into discrete small molecules, oligomers or polymers, generating new functional materials with useful mechanical, catalytic, thermal, chemical and optoelectronic properties. This review presents the contemporary research development of the field, with emphasis on the fundamental concepts, facile tuning of the photophysical properties and possible energy-related applications of various functional metal Schiff base complexes. To date, many soluble conjugated materials based on metal Schiff base complexes have been generated and studied. They have found an array of energy applications, for example, as converters for light/electricity signals in organic light-emitting diodes and dye-sensitized solar cells, energy storage and potential conductive thermoelectric materials.

Keywords	dye-sensitized solar cell; energy material; organic light-emitting diode; Schiff base; transition metal

Corresponding Author	Wai-Yeung Wong
Corresponding Author's Institution	The Hong Kong Polytechnic University
Order of Authors	Wai-Yeung Wong, Jie Zhang, Linli Xu

Suggested reviewers	Paul Raithby, Pierre D. Harvey, Tong Ren, Alaa Abd-El-Aziz, Qiang Zhao

Submission Files Included in this PDF

File Name [File Type]

response letter.doc [Response to Reviewers]

Highlights.doc [Highlights]

CCR_2017_236 submitted.doc [Manuscript File]

To view all the submission files, including those not included in the PDF, click on the manuscript title on your EVISE Homepage, then click 'Download zip file'.

Highlights

- A survey of metal Schiff base complexes for energy-related applications is provided
- The potential of using these complexes as energy materials is highlighted and discussed

Coord. Chem. Rev. **(Special Issue on "The Diversity of Coordination Chemistry" in Honor of Prof. Pierre Braunstein)**

Energy materials based on metal Schiff base complexes

Jie Zhang*[a], Linli Xu*[b], Wai-Yeung Wong*[b]

[a] *Department of Chemistry, School of Pharmaceutical and Chemical Engineering,Taizhou University, 1139 Shifu Road, Taizhou 318000, Zhejiang Province, P. R. China*

[b] *Department of Applied Biology and Chemical Technology, The Hong Kong Polytechnic University, Hung Hom, Hong Kong, P. R. China*

Received XXXXX

Corresponding author. Tel.: +852 34008670.

E-mail address: zhang_jie@tzc.edu.cn (J. Zhang), xulinli@mail.ipc.ac.cn (L. Xu), wai-yeung.wong@polyu.edu.hk (W.-Y. Wong).

Abstract

Metal Schiff base complexes represent a class of compounds that have become a field of immense interest because of their intriguing chemical and physical properties, and their wide-ranging applications in a number of scientific areas. The presence of transition metal elements with a polydentate Schiff base ligand to form metal complexes offers a good platform for combining the chemical, electronic, magnetic, optical and redox properties of metal complexes with those of the organic materials. Metal Schiff base complexes can be incorporated into discrete small molecules, oligomers or polymers, generating new functional materials with useful mechanical, catalytic, thermal, chemical and optoelectronic properties. This review presents the contemporary research development of the field, with emphasis on the fundamental concepts, facile tuning of the photophysical properties and possible energy-related applications of various functional metal Schiff base complexes. To date, many soluble conjugated materials based on metal Schiff base complexes have been generated and studied. They have found an array of energy applications, for example, as converters for light/electricity signals in organic light-emitting diodes and dye-sensitized solar cells, energy storage and potential conductive thermoelectric materials.

Keywords: dye-sensitized solar cell; energy material; organic light-emitting diode; Schiff base; transition metal

Abbreviations: A, electron acceptor; acac, acetylacetonate; Alq_3, tris(8-hydroxyquinolinato)aluminum; BAlq, bis(2-methyl-8-quinolinolato)-mono(4-phenylphenolato)aluminum; BCP, 2,9-dimethyl-4,7-diphenyl-1,10-phenanthroline; $Bepp_2$, bis[2(2'-hydroxyphenyl)pyridine]beryllium; CBP, 4,4'-bis(*N*-carbazolyl)-1,1'-biphenyl; CE, current efficiency; CIE, Commission International de L'Eclairage; CuPc, copper phthalocyanine; D, electron donor; Da = Dalton unit; DFT, density functional theory; DMF, dimethylformamide; E_g, optical bandgap; EIS, electrochemical impedance spectroscopy; E_{ox}, oxidation potential; EL, electroluminescence; ett, 1,1,2,2-ethenetetrathiolate; EQE, external quantum efficiency; FF, fill factor; FIrpic, bis(4,6-difluorophenylpyridine)(picolinate)iridium(III); FK306, iridium(III) bis[4-(*tert*-butyl)-2',6'-difluoro-2,3'-bipyridine]acetylacetonate; GPC, gel permeation chromatography; HOMO, highest occupied molecular orbital; ITO, indium-tin oxide; ICT, intramolecular charge transfer; IL, intraligand; ILCT, intraligand charge transfer; IPCE, incident photon-to-electron conversion efficiency; LC, ligand-centered; LCD, liquid crystal display; LEC, light-emitting electrochemical cell; LUMO, lowest unoccupied molecular orbital; MLCT, metal-to-ligand charge transfer; NIR, near-infrared; NPB, 4,4'-bis[*N*-(1-naphthyl)-*N*-phenylamino]biphenyl; M_n, number-average molecular weight; OEP, octaethylporphyrin; OLED, organic light-emitting diode; PBD, 2-(4-biphenylyl)-5-(4-*tert*-butylphenyl)-1,3,4-oxadiazole; PCE, power conversion efficiency; PE, power efficiency; PEDOT:PSS 3,4-poly(ethylenedioxythiophene):poly(styrenesulfonate); PF, power factor; PF2/6, poly[9,9-bis(2-ethylhexyl)fluorene]; PL, photoluminescence; PLED, polymer light-emitting diode; PMMA, poly(methyl methacrylate); PVK, poly(*N*-vinylcarbazole); salen, *N*,*N*'-bis(salicylimine)-1,2-ethylenediamine; salen-Me_4, *N*,*N*'-bis(salicylimine)-1,1,2,2-tetramethylethylenediamine; salphen, *N*,*N*'-bis(salicylimine)-1,2-phenylenediamine; salpn, *N*,*N*'-bis(salicylimine)-1,3-propanediamine; TCTA, 4,4',4''-tri(9-carbazolyl)triphenylamine; TE, thermoelectric; TEMPO, tetramethyl-1-piperidinyloxy; THF, tetrahydrofuran; UV-vis, ultraviolet-visible; M_w, weight-average molecular weight; WOLED, white organic light-emitting diode; ZFS, total zero-field splitting; Φ_{em}, photoluminescence quantum yield; λ_{max}, absorption wavelength maximum; λ_{em}, peak emission wavelength; τ, emission lifetime; J_{sc}, short-circuit current density; LT_{50}, device lifetime; V_{oc}, open-circuit voltage; S, Seebeck coefficient; T_d, decomposition temperature; σ, electrical conductivity; K, thermal conductivity.

1. Introduction

A major global problem confronting the world today is the energy crisis. While the quality of life for the humankind depends largely on the availability of energy, the world is becoming increasingly dependent on new energy sources because of the upcoming depletion of fossil fuels [1]. One of the grand challenges of this century is to develop renewable energy systems that can give efficient and effective utilization of energy. Renewable energy sources such as solar power can provide a large amount of energy and could potentially solve our immediate energy needs. There is a growing concern that combustion of fossil fuels is causing an accumulation of CO_2 in the atmosphere, leading to many detrimental effects on the environment. Recent predictions show that it is necessary to find an additional 14–20 TW by 2050 when our energy reserves based on fossil fuels are varnishing [2]. Thus, scientists are looking for other sustainable energy sources to meet our future energy demand and fight for a cleaner environment. There is much research attention in developing renewable resources and improving the technologies for energy interconversions. The transformations of light into electricity (electricity generation in photovoltaic cells) and electricity into light (light generation in light-emitting diodes) are two important interrelated areas that have attracted considerable research interest in recent years (Fig. 1) [3]. Coordination and organometallic compounds have been sought and

investigated for both of these transformations and these metal complexes and polymers will undoubtedly play key roles in the efficient production, transformation and utilization of energy [4]. The chemical and physical properties of such metal-based material can be easily fine-tuned simply by varying its chemical structure (both the metal center and/or organic ligand) to develop a suitable material to fit a particular energy application.

New functional materials with tailor-made properties, low cost and straightforward synthesis are of central importance in the topical themes of material sciences. Transition metal complexes with interesting optoelectronic properties are increasingly used in the design of novel functional molecular materials [5−10]. In general, the advantages of metalation includes (i) the capability to generate active species for charge transport through the redox activity of both the metal atoms and the organic ligand; (ii) easy fine-tuning of the highest occupied molecular orbital-lowest unoccupied molecular orbital (HOMO-LUMO) energy gap through the interaction of the d-orbitals of the transition metal with the HOMO and/or LUMO of the ligand; (iii) high diversity of the molecular framework based on the coordination number, geometry and valence shell of the selected metal atom and (iv) improvement of the solubility and ease of tuning the intermolecular π-stacking and/or metallophilicity in the solid state. Among these, metal Schiff base complexes are a broad class of

compounds that have received increasing attention due to their attractive chemical and physical properties, and their wide-ranging applications in various fields [11−13].

The class of compounds, so-called imines, are often referred to as Schiff bases, named after the German chemist Hugo Schiff. Schiff bases contain the azomethine group (-RC=N-) and are typically formed by the condensation of a primary amine with an active carbonyl compound [14]. They have drawn considerable research attention of scientists owing to the ease of synthesis and metal complexation. Transition metal complexes of N_2O_2 Schiff base derived from salicylaldehyde and diamines have attracted intense interest as a promising class of luminescent materials [12]. Among these, metalated *N*,*N*'-bis(salicylimine)-1,2-ethylenediamine (salen), **I** (abbreviated as [M(salen)]), is the prototype of this family of compounds, which are known to exhibit intriguing electroluminescent (EL) [12], nonlinear optical (NLO) [15] and catalytic properties [16,17]. Other related compounds, such as [M(salphen)] **II** (salphen = *N*,*N*'-bis(salicylimine)-1,2-phenylenediamine), [M(salpn)] **III** (salpn = *N*,*N*'-bis(salicylimine)-1,3-propanediamine) and [M(salen-Me_4)] **IV** (salen-Me_4 = *N*,*N*'-bis(salicylimine)-1,1,2,2-tetramethylethylenediamine) (Fig. 1), demonstrate the breadth of chemical structures available for this class of molecules, which possess the central N_2O_2 binding pocket formed by two imines and two phenoxides [13]. In the past few decades, because of their preparative accessibility and high thermal stability,

M(salen)-type motifs have been commonly introduced into small discrete molecules, oligomers and polymers in the hope of generating new functional materials with desired features [12,13].

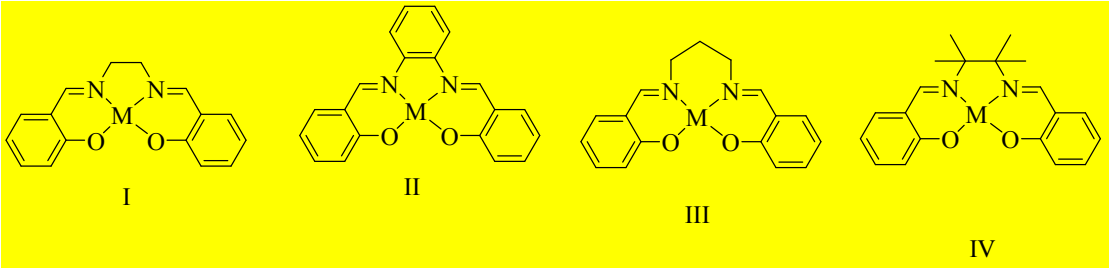

Fig. 1. Common types of metal Schiff base chromophores.

In this review, we highlight the types and photophysics of various metal Schiff base systems, with special emphasis placed on those with transition metal elements such as platinum(II), nickel(II) and zinc(II). As the synthetic chemistry of metal Schiff base complexes is prevalent, the study of their photophysical and electronic properties would provide a good access to new classes of functional molecular materials of practical interest. A survey of the reported metal Schiff base compounds for various energy-related applications is summarized here, which are useful for organic light-emitting diodes (OLEDs), dye-sensitized solar cells, energy-storing and potential thermoelectric applications.

2. Electrical to light energy conversion in organic light-emitting diodes

Recent research on organic light-emitting diodes (OLEDs) has been focused on devices composed of thin films containing organometallic molecules that can directly convert electricity into light [18−20]. OLEDs have the great potential of revolutionizing display technologies in the scientific community. The key advantages of OLEDs for flat-panel display applications are their self-emitting property, high luminous efficiency, full color capability, wide viewing angle, high contrast, low power consumption, low weight, potentially large-area color displays and flexibility [21]. They are also more energy-efficient and are generally lower in cost than liquid crystal displays (LCDs). In view of this, the rapidly growing market for OLED technology is driving both the academic and industrial sectors toward the development of new functional materials for advanced manufacturing technology. Heavy metal complexes have recently gained tremendous research interest for fabricating highly efficient phosphorescent OLEDs by taking advantage of the 1:3 exciton singlet/triplet ratio predicted by simple spin statistics [18–21]. These phosphorescent emitters are mainly derived from the family of the third-row transition metal (Re(I), Os(II), Ir(III) and Pt(II)) complexes [22–24], although examples with some second-row transition metals such as Ru(II) [22] and first-row transition metals such as Cu(I) are also known [25,26]. The three key electronic processes, namely, (i)

charge injection, (ii) charge transport, and (iii) electron-hole recombination (i.e. exciton formation) efficiency must be individually optimized in order to improve the overall OLED performance. The pioneering work by Forrest and Thompson based on the utilization of triplet emitters rather than singlet emitters was a breakthrough in tackling the recombination efficiency issue [27], and has since led to a plenty of successful research stories on phosphorescent molecules. This strategy enhances light emission efficiency by electrophosphorescence. The advantage of triplet emitters over the singlet-emitting congeners is that they can capture energy from both singlet and triplet excited states, lifting the upper limit of the internal quantum efficiency of the usual fluorescent dopant-based devices from 25% to nearly 100%. Triplet emitters with heavy metal ions allow for circumvention of this limitation if the excitons generated by hole-electron recombination reside at a site where efficient spin-orbit coupling leads to efficient singlet-triplet state mixing which eliminates the spin-forbidden nature of the radiative relaxation of the triplet state. Of all the systems investigated to date, $[Ir(ppy)_3]$ [28] and $[Ir(ppy)_2(acac)]$ [29] (ppy = 2-phenylpyridine anion, acac = acetylacetonate) are the most well-studied compounds in this area.

1 R^1 =  , R^2 = H, R^3 = H, R^4 = H, R^5 = H

2 R^1 =  , R^2 = H, R^3 = Br, R^4 = H, R^5 = H

3 R^1 =  , R^2 = H, R^3 = H, R^4 = H, R^5 = H

4 R^1 =  , R^2 = H, R^3 = H, R^4 = H, R^5 = H

5 R^1 =  , R^2 = H, R^3 = CH_3, R^4 = H, R^5 = H

6 R^1 =  , R^2 = H, R^3 = $C(CH_3)_3$, R^4 = H, R^5 = H

7 R^1 =  , R^2 = H, R^3 = F, R^4 = H, R^5 = H

8 R^1 =  , R^2 = CH_3, R^3 = H, R^4 = H, R^5 = H

9 R^1 =  , R^2 = CH_3, R^3 = H, R^4 = F, R^5 = H

10 R^1 =  , R^2 = CH_3, R^3 = OCH_3, R^4 = H, R^5 = H

11 R^1 =  , R^2 = H, R^3 = H, R^4= H, R^5 = H

12 R^1 =  , R^2 = CH_3, R^3 = $C(CH_3)_3$, R^4 = H, R^5 = H

13 R^1 =  , R^2 = H, R^3 = H, R^4 = H, R^5 = H

14 R^1 = 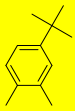 , R^2 = H, R^3 = H, R^4 = H, R^5 = H

15 R^1 =  , R^2 = H, R^3 = H, R^4 = H, R^5 = H

16 R^1 =  , R^2 = H, R^3 = F, R^4 = H, R^5 = H

17 R^1 =  , R^2 = H, R^3 = H, R^4 = COOMe, R^5 = H

18 R^1 =  , R^2 = H, R^3 = H, R^4 =  , R^5 = H

19 R^1 =  , R^2 = H, R^3 = H, R^4 = , R^5 = H

20 R^1 =  , R^2 = H, R^3 = $C(CH_3)_3$, R^4 = H, R^5 = $C(CH_3)_3$

21 R^1 =  , R^2 = H, R^3 = $C(CH_3)_3$, R^4 = H, R^5 = $C(CH_3)_3$,

22 R^1 = 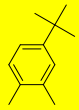 , R^2 = H, R^3 = $C(CH_3)_3$, R^4 = H, R^5 = $C(CH_3)_3$,

23 R^1 =  , R^2 = H, R^3 =  , R^4 = H, R^5 = H

24 R^1 = 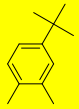 , R^2 = H, R^3 =  , R^4 = H, R^5 = H

25 R^1 =  , R^2 = H, R^3 = $C(CH_3)_3$, R^4 = H, R^5 = $C(CH_3)_3$

26 R^1 =  , R^2 = H, R^3 = Br, R^4 = H, R^5 = $C(CH_3)_3$

27 R^1 =  , R^2 = H, R^3 = $C(CH_3)_3$, R^4 = H, R^5 = $C(CH_3)_3$

28 R^1 =  , R^2 = H, R^3 = H, R^4 = H, R^5 = H

29 R^1 = 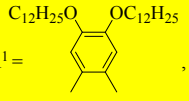 , R^2 = H, R^3 = $C(CH_3)_3$, R^4 = H, R^5 = $C(CH_3)_3$

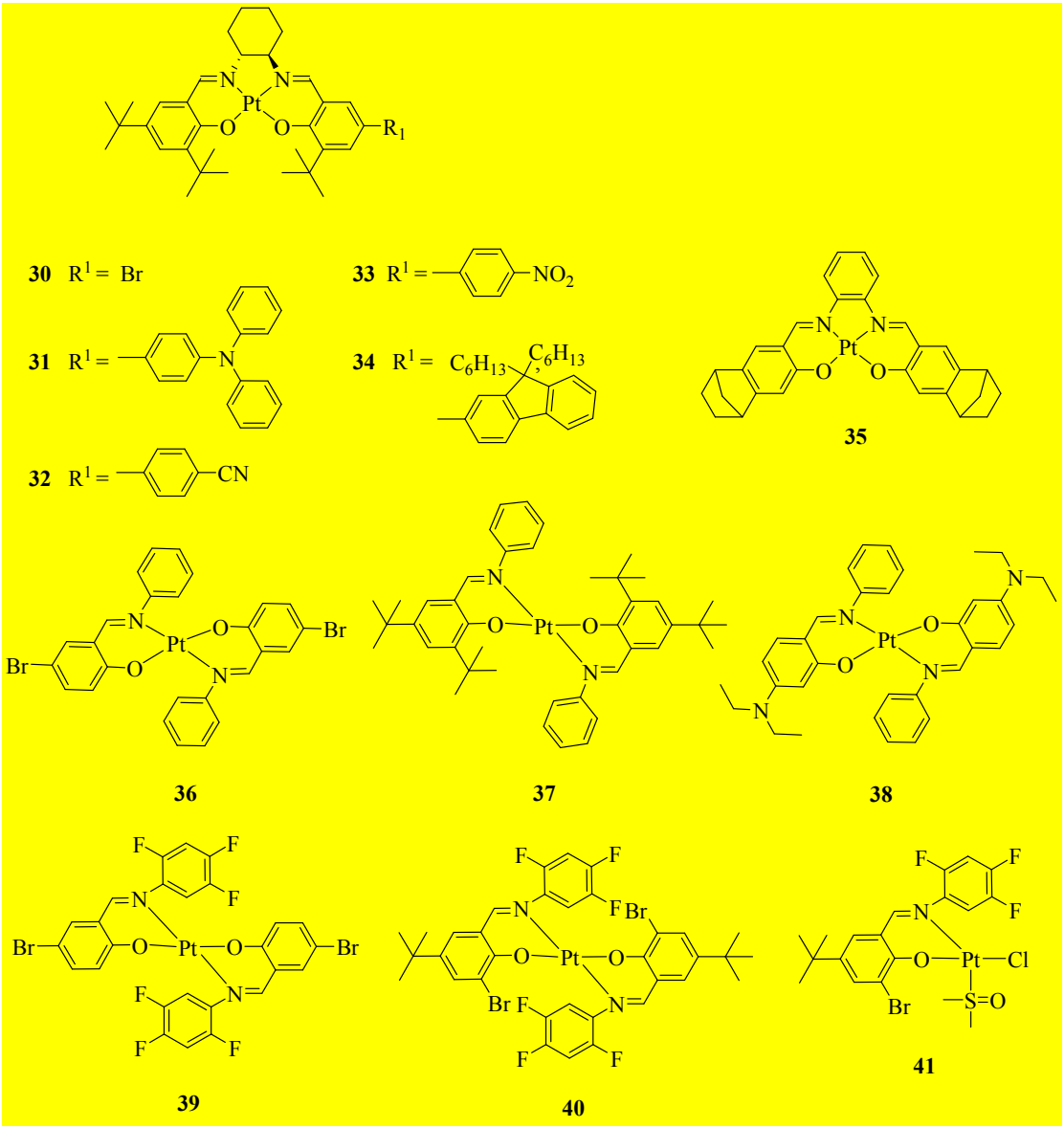

2.1 Discrete mononuclear metal Schiff base complexes

It was demonstrated that Pt(II) Schiff base complexes (e.g. **1**–**41**) constitute an attractive class of phosphorescent materials that are easily synthesized and structurally modified, thermally stable and potentially important in OLED applications (Tables 1 and 2). Che et al. have pioneered the EL studies of phosphorescent d^8 Pt(II) Schiff base complexes and have communicated that these complexes can be used for high-performance OLEDs. Following this, a series of phosphorescent Pt(II) Schiff base

complexes **1**−**16** has been synthesized and fully characterized, and their applications in OLEDs have been reported in detail [31]. They are easily prepared by a one-pot reaction. They are typically stable toward air and moisture, have a high decomposition temperature and are strongly phosphorescent. Detailed investigations of the photophysical properties of these Pt(II) complexes were also presented [31]. The low-energy absorption bands of these complexes are assigned to metal-to-ligand charge-transfer (MLCT): ^{1}[Pt(5d)→π*(Schiff base)] character mixed with ^{1}[lone pair(phenoxide)→π*(imine)] charge-transfer character. This assignment is in good agreement with the significant MLCT perturbation in the triplet state as revealed by the total zero-field splitting (ZFS) values obtained (ca. 14–28 cm^{-1}). ZFS can be used to estimate the extent of MLCT perturbation and spin-orbital coupling efficiency of the emitting triplet excited state and to assess the suitability of an emitter in fabricating OLEDs [32−35]. In general, the higher the ZFS value, the more metal d-orbital involvement is present in the triplet excited state. This reduces the energy difference between the excited singlet and triplet states, enhances the singlet-triplet intersystem crossing rate and lowers the emission decay lifetime. The total ZFS for **4** was estimated to be 20 cm^{-1} and the triplet emitting state exhibited intraligand charge transfer (ILCT) character with significant MLCT perturbation. For **1**–**18**, intense phosphorescence emission bands with λ_{em} at 541–592 nm (Φ_{em} = 7–26%, τ = 0.46–3.5

μs) are observed upon photoexcitation and the emission lifetimes are shorter as compared to those of Pt(II) octaethylporphyrin (PtOEP, typically > 50 μs) [27]. Complex **16** shows the highest photoluminescence (PL) quantum yield. The time-resolved absorption spectrum of the emissive triplet excited state of **4** in degassed CH_3CN features an absorption band at about 480 nm, and the measured decay lifetime of 3.6 μs closely matches the emission lifetime in CH_3CN, suggesting that the emission band originates from the triplet excited state. Replacing the ethylene bridge of the Schiff base ligand with a π-conjugated phenylene ring leads to a red-shifted emission. This is consistent with the theoretical studies [36]. Complexes **11**–**16** with phenylene R^1 skeleton display a red phosphorescence emission with λ_{em} at 610–649 nm (Φ_{em} = 7–27%, τ = 2.87–4.62 μs) in CH_3CN at 298 K. Self-quenching of the emission bands of **1**–**16** with concentrations from 1×10^{-5} to 5×10^{-3} mol dm^{-3} occurs in solution. The device performances using different Pt(II) Schiff base complexes as electrophosphorescent dopants are summarized in Table 2. Devices with the best performances were typically obtained at low dopant concentrations for these complexes. The EL spectra of all the devices match the PL spectra of the corresponding complexes, which indicates that all EL emissions come directly from the triplet excited states of the Pt(II) complexes. The devices fabricated from **1**–**8** gave orange EL emission, which can afford a white light by a combination with the blue

light. For instance, by using **1** and bis[2(2'-hydroxyphenyl)pyridine]beryllium) ($Bepp_2$) as emitters, a white organic light-emitting diode (WOLED) with Commission International de L'Eclairage (CIE) coordinates of (0.33, 0.35) was obtained [30]. Also, an optimized OLED doped with 4 wt% **4** showed a peak external quantum efficiency (EQE), current efficiency (CE) and power efficiency (PE) of 11%, 31 cd A^{-1} and 14 lm W^{-1}, respectively. A red OLED doped with **11** also afforded promising device performance at 9.4% and 4.9 lm W^{-1}, showing initially a lifetime of >20,000 h at 100 cd m^{-2} and an even better value of 77,000 h at 500 cd m^{-2} by modifying the device configuration. Devices fabricated with **11**–**14** produced red emission bands with the CIE coordinates at (0.65, 0.34), which are close to the red color of the National Television Standards Committee (NTSC) (1979) standard for the cathode ray tube. Complex **11** afforded device with the best performance, showing maximum EQE and PE at 9.4% and 4.9 lm W^{-1}, respectively and a device lifetime of > 20,000 h at 100 cd m^{-2}. It was also shown that by inserting a hole injection layer of copper phthalocyanine (CuPc) between the indium-tin oxide (ITO) and 4,4'-bis[*N*-(1-naphthyl)-*N*-phenylamino]biphenyl (NPB) layers, the hole injection barrier was lowered which can improve the device lifetime to 77,000 h at 500 cd m^{-2} [30]. This lifetime can fulfil the basic requirement for use in the display panels of mobile phones, MP3 players and televisions.

A systematic investigation on the emission efficiency of a group of d^8 transition-metal Schiff base complexes was also performed by Che and co-workers which allows us to understand the different photophysics of $[M(salen)]_n$ complexes (M = Pt, Pd, n = 0; M = Au, n = +1) in CH_3CN solutions at room temperature. While [Pt(salen)] is phosphorescent and [Pd(salen)] is fluorescent, $[Au(salen)]^+$ is non-emissive [36]. A detailed theoretical analysis on **11**, **12** and **17** was also undertaken in order to study the effects of Schiff base substituent(s) on the radiative and non-radiative decay rates.

Another three Pt(II) complexes **18**–**20** based on donor-π-acceptor (D-π-A) Schiff base ligands were also described, in which the strong electron-withdrawing units such as dicyanovinyl and (trifluoromethyl)phenyl moieties and electron-donating units such as 4-diethylaminophenyl and 3,5-di(*tert*-butyl)phenyl groups can fine-tune the emission wavelength from yellow to red and somewhat improve the Φ_{em} [37]. In other words, such D-π-A configurations with efficient intramolecular charge transfer (ICT) can effectively modulate the HOMO and LUMO energy levels. The decay times in the microsecond scale (1.97–2.35 μs) indicate their phosphorescence origin from the triplet excited state. The B3LYP density functional theory (DFT) calculations are in good agreement with their photophysical properties. Thanks to its deep-red emission color, complex **21** was also developed and used as a dopant in tris(8-

hydroxyquinoline)aluminum (Alq_3) for the fabrication of OLEDs [38]. The results were also compared to the related complex **11**. The X-ray crystal structure of **21** reveals that the sterically bulky *tert*-butyl groups can hinder the stacking of molecules. A stable red color with CIE coordinates of (0.69, 0.30) was obtained in the **21**-based OLEDs, showing an impressive EQE of 21%. A better EL performance of **21** over **11** is attributed to the reduction of the aggregation-induced quenching in the presence of the *tert*-butyl substituents for the former case.

It was found that the formation of aggregate/excimer would reduce the emission efficiency and color purity of the Pt(II) salen and salphen Schiff base complexes when they were at high concentrations. This phenomenon can be ascribed to the triplet-triplet annihilation, Pt···Pt and π-π interactions at the high concentration in the solid state. A series of thermally stable symmetric and asymmtric Pt(II) Schiff base complexes containing bulky *tert*-butyl and triphenylamino substituents **25**–**34** were also prepared which can reduce the aggregation or excimer formation [39]. The absorption spectra of these complexes are shown in Fig. 2. In CH_2Cl_2, the spectra of **25**, **26** and **30**–**34** , having the aliphatic R^1 unit, are similar to each other. Each of them shows strong high-energy absorption bands at λ_{max} = 253–352 nm and moderately intense absorption bands at λ_{max} = 425–441 nm due to intraligand (IL) π-π* and MLCT mixed with IL transitions (*vide supra*). Complexes **27**–**29** with the

phenylene R^1 motif display two high-energy absorptions at λ_{max} = 368–393 nm and moderately strong absorption bands at λ_{max} = 476–555 nm, which are red-shifted relative to the cases with the aliphatic R^1 segment, again thanks to the expansion of the π-conjugation. The absorptions of these metal Schiff base complexes are quite similar, which indicate that the substituents on the Schiff base ligands only have a minimal effect on the absorption energy. The PL spectra of **25**–**34** are depicted in Fig. 3. Intense emission bands are observed at λ_{em} = 557–568 nm (Φ_{em} = 11–20%; τ = 2.60–12.80 μs) for **25**, **26**, **30**, **31**, **32** and **34** in CH_2Cl_2 whereas **33** gives very weak emission at 556 nm (Φ_{em} = 0.71%) due to the presence of the electron-deficient nitro moiety. Complexes **27** and **29** display red PL maxima at 650 and 649 nm, respectively (Φ_{em} = 12 and 11%; τ = 2.60 and 2.85 μs). Complex **28** bridged by the pyridyl R^1 group shows an emission signal at λ_{em} = 612 nm (Φ_{em} = 17%; τ = 7.72 μs, respectively). Using **25**, **26** and **31** as phosphorescent dyes, yellow OLEDs were fabricated with improved efficiency as compared to other reported Pt(II) analogues [40]. Unlike other typical Pt(II) dopants, in which the EL was found to display remarkable spectral shifts upon dopant aggregation to give a broad red-shifted excimer emission [41], the EL spectra using **25** or **31** as dopant are shown to be independent of the driving voltage from 4.5 to 15 V (Fig. 4) and dopant concentration. The voltage-independent EL spectra is attributed to the inhibition of **25** or **31** to form

aggregates via Pt···Pt and/or π-π stacking interactions in the thin films [39]. Device doped with 8 wt% **31** in 4,4',4''-tri(9-carbazoyl)triphenylamine (TCTA) furnished λ_{em} at 564 nm, maximum CE of 23 cd A^{-1}, PE of 17 lm W^{-1} and luminance of 11,106 cd m^{-2}. Moreover, a single-layer WOLED consisting of **31** and blue-emitting bis(4,6-difluorophenylpyridine)(picolinate)iridium(III) (FIrpic) was fabricated which afforded a white light with the CIE coordinates of (0.34, 0.44) at 9 V and peak EQE, CE and PE of 7.7%, 21 cd A^{-1} and 17 lm W^{-1}, respectively (Fig. 5) [39].

Unlike octahedral cyclometalated iridium(III) phosphors, the planar coordination geometry of Pt(II) complexes usually favors intermolecular ligand-ligand and/or metal-metal interactions. The presence of such intermolecular interactions facilitates the formation of low-lying aggregation states, resulting in the quenching of emission(s) in most cases, and hence, poses a detrimental effect on both the efficiency and color purity of the OLEDs. Another common shortcoming of Pt(II) phosphors is their relatively long emission lifetimes relative to those of the Ir(III) phosphors. In this context, a series of sterically hindered red-emitting Pt(II) Schiff base complexes **21**–**24** and **35** with narrow optical bandgaps (E_g) were prepared and the results were compared to those of complex **11** [42]. These bulky complexes emit red color light in the range of 624–643 nm with Φ_{em} = 6–20% and τ = 3.5–6.3 μs (versus 618 nm, 20% and 3.6 μs for **11**). Complex **35** shows a significantly mitigated emission self-

quenching rate constant of 1×10^7 M^{-1} s^{-1} and a significant delay of efficiency roll-off, owing to the presence of a rigid three-dimensional bulky norbornene groups in the ligand scaffold. A high doping concentration of **35** can be used in the OLED devices without deteriorating the device performance, hence allowing more complete energy transfer from the host to the emitter. Red electrophosphorescence with a high EL efficiency was realized by doping **35** into host materials with stepwise energy levels [42]. This is caused by the reduced self-aggregation, improved carrier trapping ability of **35** and optimization of the double emissive layer device structure. Co-doping a low level of FIrpic or iridium(III) bis[4-(*tert*-butyl)-2',6'-difluoro-2,3'-bipyridine]acetylacetonate (FK306) into the electron-dominant emissive layer was able to improve the EL performance by enhancing the carrier balance, broadening the recombination zone and facilitating the energy transfer from the host to the emitter. Compared with the control devices, the co-doped devices gave higher efficiency and luminance, slower roll-off of EL efficiency and improved device lifetime. The peak EQE, CE and PE were 11.7%, 20.4 cd A^{-1} and 18.3 lm W^{-1}, respectively, and the OLED showed a projected device lifetime (LT_{50}) of 18,000 h.

A series of *trans*-bis(salicylaldiminato) Pt(II) complexes (i.e. one-armed metal Schiff base complexes) **36**–**41** was also nicely developed and fully characterized by spectroscopic and crystallographic methods [43]. They can be easily prepared through

1:1 condensation of salicylaldehyde and monoamine, and show better flexibility and lower conjugation length than salen and salphen types of Schiff bases, which may cause a blue-shifted emission accordingly. These complexes with different electron-withdrawing and -donating groups display green to orange phosphorescence in the solid state. Blue to orange emitting OLEDs were achieved with moderate efficiency values.

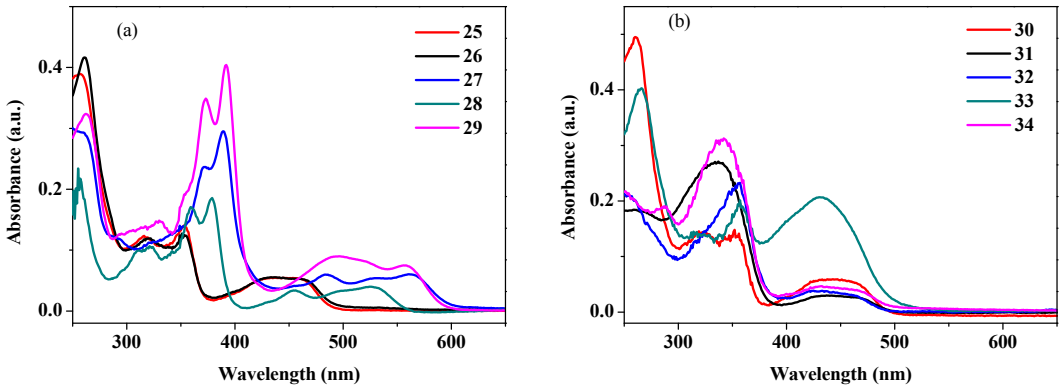

Fig. 2. UV-vis absorption spectra of Pt(II) Schiff base complexes (a) **25**–**29** and (b) **30**–**34** in CH_2Cl_2 (1.0×10^{-5} M) at room temperature.

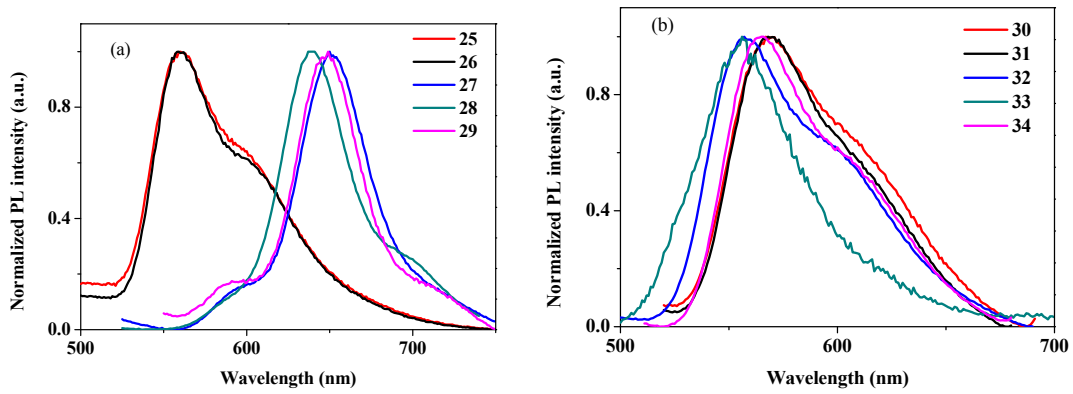

Fig. 3. Emission spectra of Pt(II) Schiff base complexes (a) **25**–**29** and (b) **30**–**34** in CH_2Cl_2 (1.0×10^{-5} M) at room temperature.

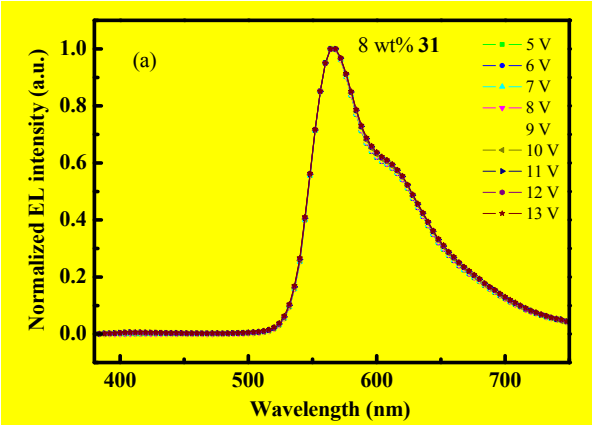

Fig. 4. Representative EL spectra of the OLED fabricated with 8 wt% **31** at the driving voltage from 5 to 13 V.

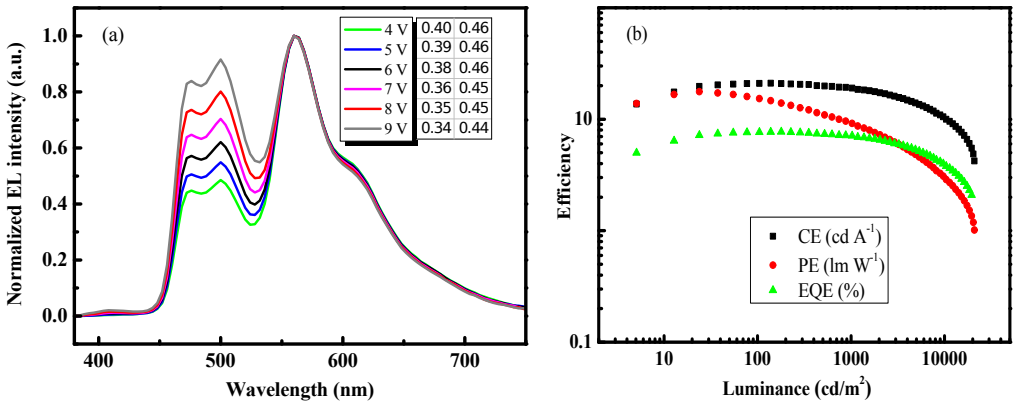

Fig. 5. Performance of WOLED using a single emissive layer of dopants **31** and FIrpic: (a) EL spectrum; (b) power efficiency-luminance, luminance efficiency-luminance and external quantum efficiency-luminance curves.

An interesting class of phosphorescent Pt(II) complexes supported by tetradentate bis(pyrrole)-diimine ligands **42**–**44** was also reported in 2005 [44]. Among these complexes, the PL spectrum of **44** occurs at the lowest energy, presumably due to its extended π-conjugated ligand system. Complex **42** shows a yellow emission at 566 nm (with a shoulder peak at 613 nm) in dilute CH_3CN with Φ_{em} = 9.7% and τ = 4.2 μs, respectively. At elevated concentrations in either solution

or 4,4'-bis(*N*-carbazolyl)-1,1'-biphenyl (CBP) film, complex **42** gives a red-shifted emission at 610 nm due to the excimer or oligomer formation at high concentration. Complex **43** shows Φ_{em} = 10.5% and τ = 3.6 μs in CH_3CN. There is no excimer or oligomer emission in the case of **43**, because the methylene group of **43** presumably did not favor close intermolecular contacts. Since complex **44** shows emission close to the near infrared (NIR) region with low Φ_{em} (0.10%), phosphorescent OLEDs have been fabricated only for the former two dyes **42** and **43**. OLEDs based on 6 wt% **42** gave a red EL peak at 620 nm with the CIE coordinates of (0.62, 0.38) and the peak EQE, CE and PE were 6.5%, 9.0 cd A^{-1} and 4.0 lm W^{-1}, respectively. Respectably high efficiencies (5.2%, 7.7 cd A^{-1} and 2.4 lm W^{-1}) were still observed even at a high luminance of 5,000 cd m^{-2}. This device performance is very attractive for red OLEDs based on Pt(II) emitters in the literature and represents a good platform to show that excimer formation of Pt(II) complexes can also lead to an efficient low-energy red emission. The corresponding orange-emitting OLEDs based on **43** did not exhibit red-shifted EL at high doping levels and gave decent peak efficiencies of 4.9%, 13.1 cd A^{-1} and 5.9 lm W^{-1}.

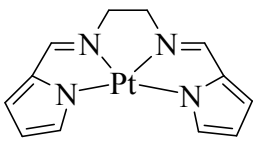

42

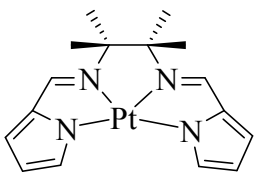

43

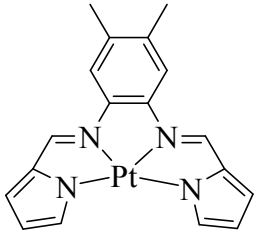

44

On the other hand, the EL behavior of Zn(II) Schiff base complexes have also been investigated since 1993. Hamada et al. pioneered the development of Zn(II) complexes bearing 2:1 bidentate azomethine (**45**) and 1:1 tetradentate N_2O_2 Schiff base ligands (**46**) and they can be used to fabricate blue OLEDs [45]. Liu and co-workers also reported a blue-emitting Zn(II) complex (**47**) [46]. However, in contrast to the Pt(II) Schiff base complexes, Zn(II) Schiff base complexes normally only emit from the singlet excited state with low Φ_{em}.

Lepnev and co-workers have intensively studied the PL and EL properties of a group of Zn(II) Schiff base complexes **48**–**51** [47]. The luminescence instability of the thin films and the fabricated OLEDs have been carefully investigated [48]. There is evidence that long heating and exposure to intense UV light leads to irreversible degradation but a weak UV light does not cause any noticeable degradation. This is promising for OLED operation under day light. In order to stabilize the OLED operation, precautions are needed to avoid humidity during OLED fabrication and encapsulation. Later on, the same research group studied the mechanisms of EL degradation in detail [49], in which the devices were shown to undergo reversible and irreversible mechanisms of degradation. The reversible one is mainly related to the charge carrier trap filling. Also, various mechanisms of irreversible degradation were observed under UV light irradiation, heating and ageing under ambient conditions.

The degradation mechanisms of OLEDs under heating from 293 to 320 K were associated with the changes in the interface regions. The initial degradation can be relieved by applying an alternating bias voltage, decreasing the substrate temperature and velocity of the thermal evaporation of materials. It was reported that the OLED performance of **48** was improved by using an insert layer structure in the two-unit stacked OLEDs [50]. The insert electrode layers comprising LiF (1 nm)/Al (5 nm) are used as a single semi-transparent mirror and bilayer cathode LiF (1 nm)/Al (100 nm) is used as a reflecting mirror. The two mirrors form a Fabry-Perot microcavity and two emissive units. Due to its microcavity effect, the intercalation device gives an overwhelmingly better performance, including better color purity, EL intensity and efficiency, than the device without intercalation and the best CE is 2.65 cd A^{-1}. Complex **52** showing D-A type ICT was also developed as a sublimable highly fluorescent red dye for high-performance OLEDs [51]. It emits at 580 nm (Φ_{em} = 67%) in CH_3CN which overlaps well with the emission peak of Alq_3. The OLEDs afforded very bright saturated red emission with CE of 0.46 cd A^{-1} at 20 mA cm^{-2} and CIE coordinates of (0.67, 0.32). Two blue-emitting fluorescent complexes **53** and **54** bearing Schiff base-containing calixarene ligands were also isolated and the authors believed that they are prospective OLED materials [52]. They emit at 450 and 485 nm, respectively. Yu et al. reported in two papers that two structurally similar

complexes **55** and **56** with the flexible chain in the Schiff bases are blue emitters and their OLEDs show EL peaks at 450 and 455 nm, respectively [53,54]. They are superior to the aromatic bridged ones in terms of solubility and processability for OLED fabrication. For **55**, the device turned on at 4.5 V and gave a peak EQE of 1.27 cd A^{-1} [43]. The best device based on **56** showed the turn-on voltage at 5 V and the maximum CE of 0.63 cd A^{-1} was obtained [54].

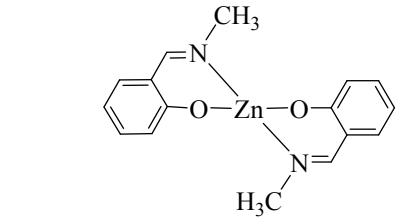

45

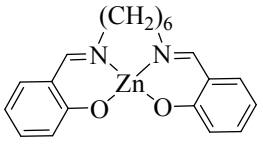

46

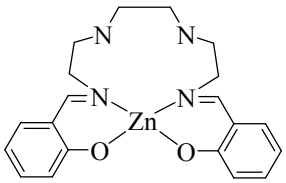

47

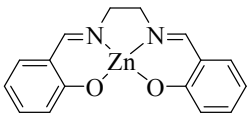

48

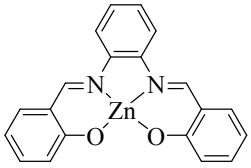

49

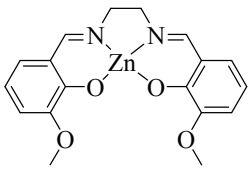

50

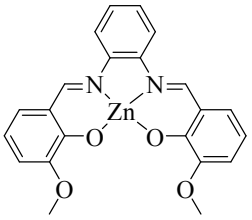

51

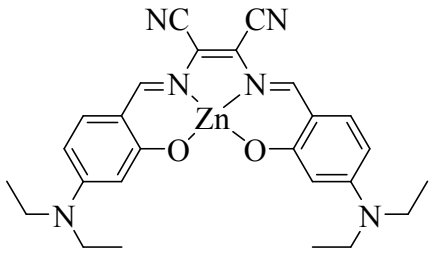

52

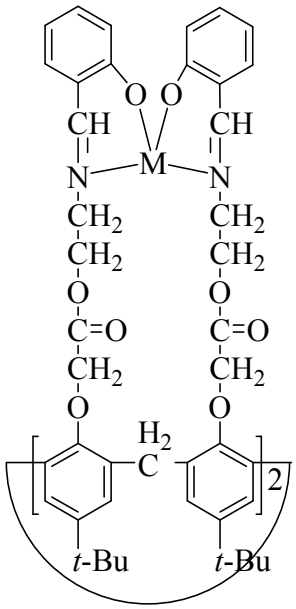

M = Zn, **53**
M = Be, **54**

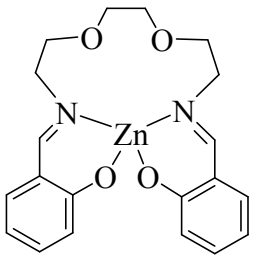

55

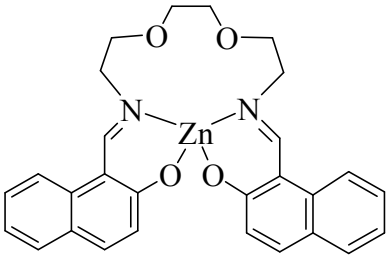

56

New air-stable aluminum(III)-salen complexes **57**–**60** were synthesized by Do et al. and their respective 5 wt% decomposition temperatures (T_d) are 230, 270, 280 and 330 °C, indicative of an increased chemical stability from **57** to **60** [55]. The absorption and PL wavelength maxima at 364 and 480 nm, respectively, are very close to each other for them regardless of the type of the ancillary aryloxy ligand used. These Al(III) complexes have Φ_{em} in the range of 31–41%. Complex **60** was selected and confirmed to be a better hole-blocking material for phosphorescent OLEDs than bis(2-methyl-8-quinolinolato)-mono(4-phenylphenolato)aluminum (BAlq). Under the same device configuration using the green phosphorescent dopant [$Ir(ppy)_3$], the device based on **60** emitted a stable green light with CE of 17.1 cd A^{-1} and PE of 4.7 lm W^{-1} at 20 mA cm^{-2} but BAlq only gave CE of 12.3 cd A^{-1} and PE of 3.6 lm W^{-1}. On the other hand, three more Al(III)-salen complexes **61**–**63** were

reported by the same research group in which complex **63** can act as an unprecedented multifunctional light-emitting materials for host-dopant assembled OLEDs fabricated by solution processing [56]. Direct molecular coupling of an Al(III)-salen complex (as the host) and a charged Ir(III)-phenylpyridine complex (as a phosphorescent emitter) gives rise to the heterodinuclear complex **63**. Complexes **61** and **62** essentially were prepared as the control compounds for comparison in such study. By using the host-dopant assembly protocol, the drawbacks of phase seaparation and excimer formation associated with the spin-coating approach of blends of phosphorescent metal complexes and host polymers can be avoided. Thus, the OLED based on **63** can offer very good performance at EQE = 0.94%, CE = 1.8 cd A^{-1} and PE = 0.69 lm W^{-1}. The low turn-on voltage of 3.4 V, owing to the good charge transport feature of the device arising from the ionic nature of the complex, is also a good reflection of the beauty of such host-dopant system.

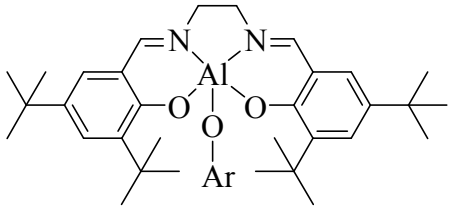

Ar = C_6H_5 **57**
= *p*-C_6H_4(OMe) **58**
= C_6F_5 **59**
= *p*-$C_6H_4(C_6H_5)$ **60**

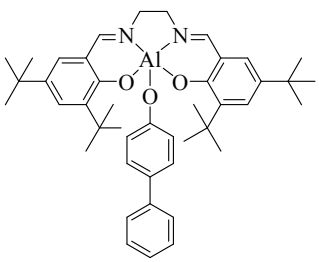

61

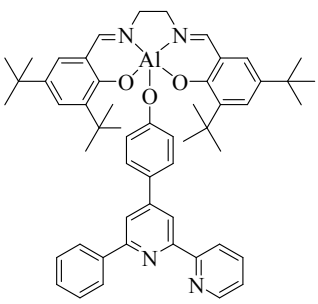

62

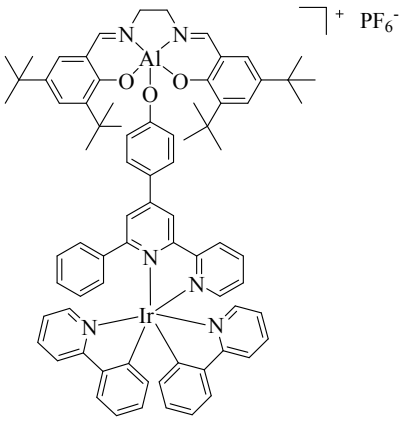

63

2.2 Metallopolymers

Metal Schiff base chromophores can also be incorporated into the polymeric scaffolds to make polymer light-emitting devices (PLEDs). PLEDs are widely considered as candidates in large-area displays and solid-state lighting sources given their prominent advantages such as flexibility, low driving voltage, light weight, simple fabrication process, etc. [57]. Some high-molecular-weight Pt(salen)-fluorene copolymers **64** and **65** were synthesized by the Ni(0)-mediated Yamamoto-type coupling reaction between a dichloro-substituted Pt(salen) complex and 2,7-dibromo-9,9-dialkylfluorene [58]. The copolymer **64** shows an intense absorption at 383 nm due to the polyfluorene segment and a low intensity absorption shoulder at 450 nm due to the [Pt(salen)] unit. The solid-state PL spectrum of **64** displays a red-shifted polyfluorene emission (peaking at 428 nm) and a lower energy PL peak at 575 nm due to the phosphorescence of the [Pt(salen)] complex, and reveals that significant energy transfer from the excited polyfluorene unit to the green-emitting [Pt(salen)]

phosphor. The PLED based on **64** gives a main EL peak at 640 nm with very low CE of 0.1−0.3 cd A^{-1}. Next, by blending copolymer **65** with poly(9-vinylcarbazole) (PVK) and 2-(4-biphenylyl)-5-(4-*tert*-butylphenyl)-1,3,4-oxadiazole (PBD) in a ratio of 4:1, the phosphorescence closely resembles the PL of [Pt(salen)] but the energy transfer between PVK and **65** is, however, rather inefficient. If the matrix becomes poly[9,9-bis(2-ethylhexyl)fluorene] (PF2/6), the PLEDs show a much more efficient energy transfer and the CE can be boosted to 3−6 cd A^{-1}. Such enhancement is believed to be caused by the reduction of the electronic interaction between [Pt(salen)] phosphor molecules (excimer formation) in the PF2/6-blended device.

Some phosphorescent conjugated oligomers (**66**−**67**) [59] and polymers (**68**−**71**) [60] consisting of alternating *p*-phenylene-ethynylene and [Pt(salphen)] units were reported. For the polymers, both linear-rod (*para*-like) and coilable (*meta*-like) structures were synthesized by the Pd(0)-catalyzed Sonogashira coupling of the appropriate diiodo-[Pt(salphen)] monomers and diethynylarene derivatives. It is shown that different emission properties are observed for *n*-alkoxy and acetylated glucosyl substituents. Initial sensing studies were carried out and analyte selectivity may be obtained by choosing suitable receptor groups.

A large series of fluorescent conjugated polymers **72** from a combinatorial synthesis and screening method was also reported by Lavastre et al. [61]. They were

similarly prepared as above by using the Pd(0)-catalyzed coupling procedure. These polymers showed high Φ_{em}, which may be suitable for PLED applications. However, they are poorly soluble in organic solvents. Following this, soluble polymer derivatives **73** were also made by MacLachlan and co-workers [62]. Long alkoxy chain substituents were introduced to both the salphen and diethynylarene monomers to increase the polymer solubility, rendering red free-standing films of high molecular weight (weight-average molecular weight M_w ca. 17,000−84,000 Da, as measured by gel permeation chromatography (GPC)). However, these copolymers do not display good emission properties in solution and energy transfer from the polymer absorption into the localized states of the metal complexes probably accounts for this. Another conjugated hyperbranched manganese(II) Schiff base polymers **74** were also synthesized by Gothelf et al. from the one-pot condensation of an aromatic trialdehyde and the corresponding diamines [63].

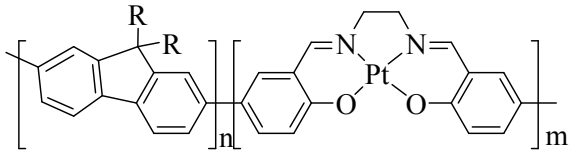

64 (R = ethylhexyl)
65 (R = octyl)

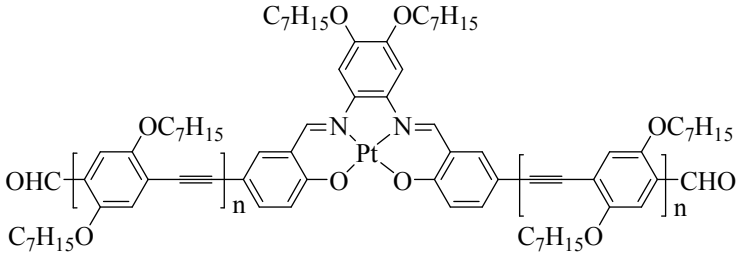

n = 1 **66**
n = 2 **67**

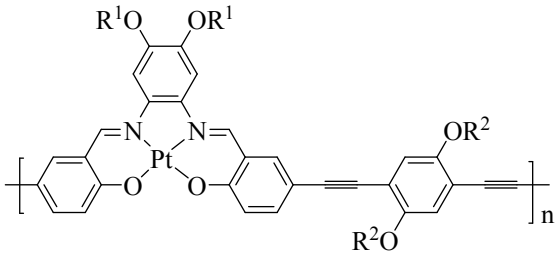

$R^1 = C_{12}H_{25}$, $R^2 = C_{16}H_{33}$ **68**

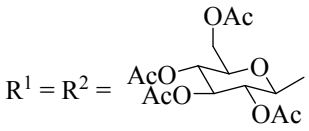

69

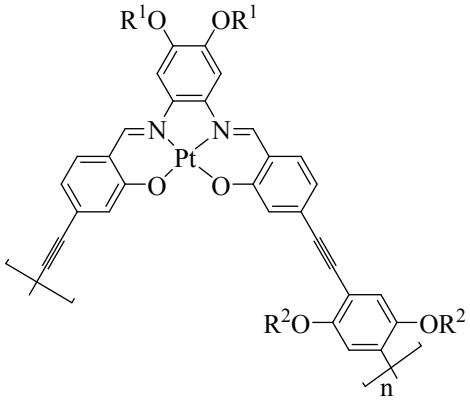

$R^1 = C_{12}H_{25}$, $R^2 = C_{16}H_{33}$ **70**

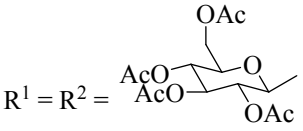

71

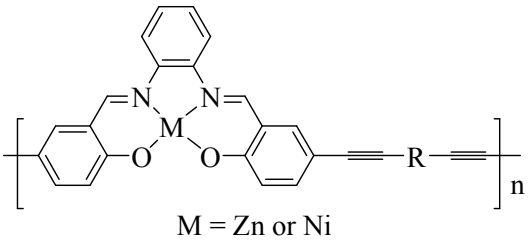

M = Zn or Ni

72

R = 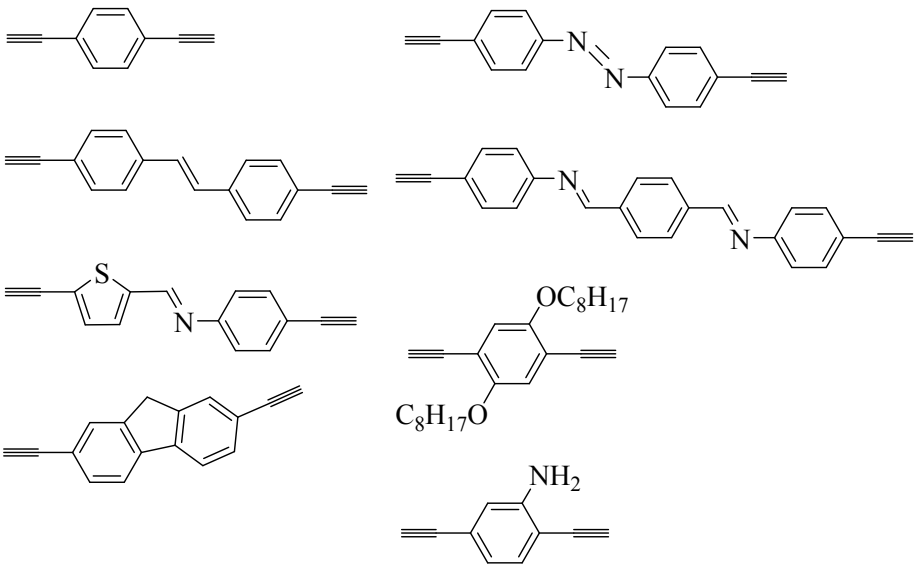

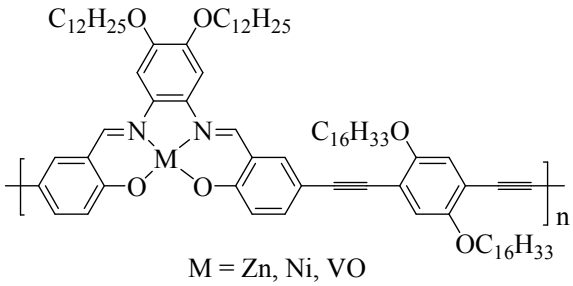

M = Zn, Ni, VO

73

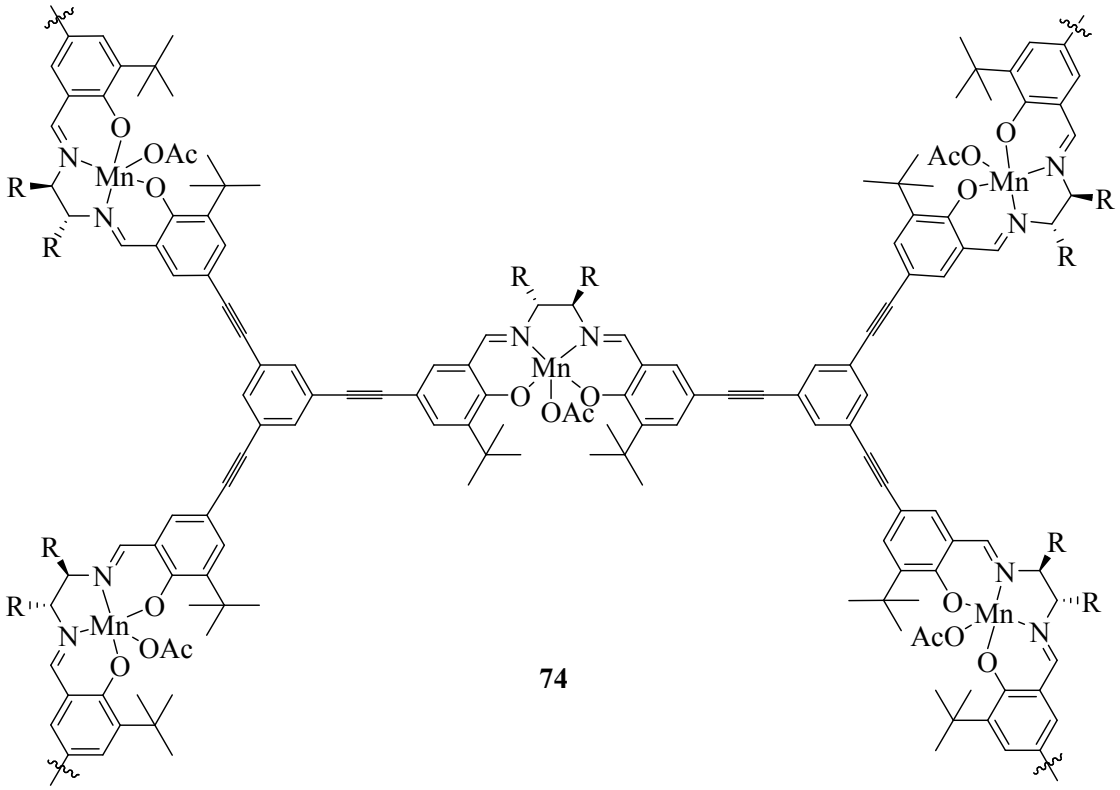

74

A family of thermally stable and structurally diverse self-assembled Zn(II) Schiff base polymers **75**−**82** were reported by Che and co-workers [64]. They were easily made by the self-assembly reactions of Zn(II) salts and salicylaldimine monomers in DMF. The number-average molecular weight (M_n) of these polymers ranges from 13,580 to 20,440, as estimated by GPC. The polymers show similar absorption features in DMF with the strong ligand-centered (LC) π-π* transitions of the *p*-phenyl

ring and salicylaldimine ligand below 400 nm together with the lowest-energy bands at 408−427 nm. They emit from blue to yellow in DMF due to the IL $^1(\pi\text{-}\pi^*)$ fluorescent emission. The emission color can be tuned by changing the R groups in the polymers and the Φ_{em} value varies from 2 to 34%. While excimer formation due to the π-π aromatic stacking interaction is evident in the film state of **81**, the presence of the bulky *tert*-butyl groups in **77** can inhibit aggregation of the polymer chains and suppresses the excimer formation effectively. Multi-layered PLEDs with the configuration of ITO /PEDOT:PSS (3,4-polyethylenedioxythiophene:polystyrenesulfonate, 30 nm)/Zn(II) polymer (30−50 nm)/BCP (2,9-dimethyl-4,7-diphenyl-1,10-phenanthroline, 20 nm)/Alq_3 (20 nm)/LiF (0.5 nm)/Al (200 nm) fabricated from **77** and **81** showed green and orange emissions, respectively, with the corresponding peak CE of 2.0 and 2.6 cd A^{-1}. In a related context, three soluble supramolecular polymers based on [Zn(salen)] chromophores **83**−**85** were reported by Cao et al. They showed good thermal stability (T_d ~311−386 °C) and emitted strong green PL emission with their λ_{em} from 531 to 546 nm (Φ_{em} = 42−51%). PLEDs based on **83**−**85** afforded green light with maximum CE of 0.9−2.3 cd A^{-1}. Two copper(I)-based photoluminescent conjugated metallopolymers **86** and **87** were also reported by Nitschke and co-workers [66,67]. They consist of a conjugated polymer backbone with each Cu(I) center bonded to the diimine moiety

and two phosphine groups (i.e. forming a Cu(N^N)P_2 core). They were shown to be temperature-responsive materials. Both polymers exhibit sol-to-gel transition upon increasing the temperature. For **86**, the polymer showed PL peak at 525 nm and 673 nm due to the IL and MLCT excited states, respectively. When the temperature became higher, the MLCT-based emission band was preferentially quenched, which was followed by a sharp color change from orange to green [66]. Polymer **87** displayed a blue-shift of λ_{em} from 780 to 580 nm when the temperature increased. Similar phenomenon was also observed from its light-emitting electrochemical cells (LECs) in which the polymer emitted infrared light at low voltage but a yellow light at higher voltage. The process can be reversed over time by lowering the voltage. The mechanism for this responsive behavior is attributed to the loss of Cu(I) phosphine core from the polymer [67].

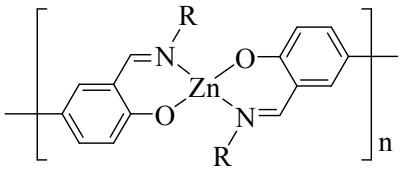

R =

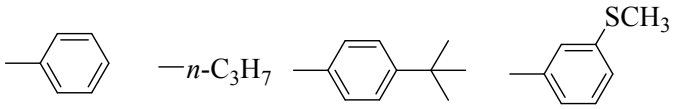

75 **76** **77** **78**

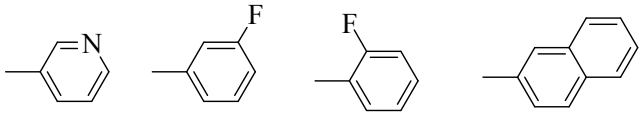

79 **80** **81** **82**

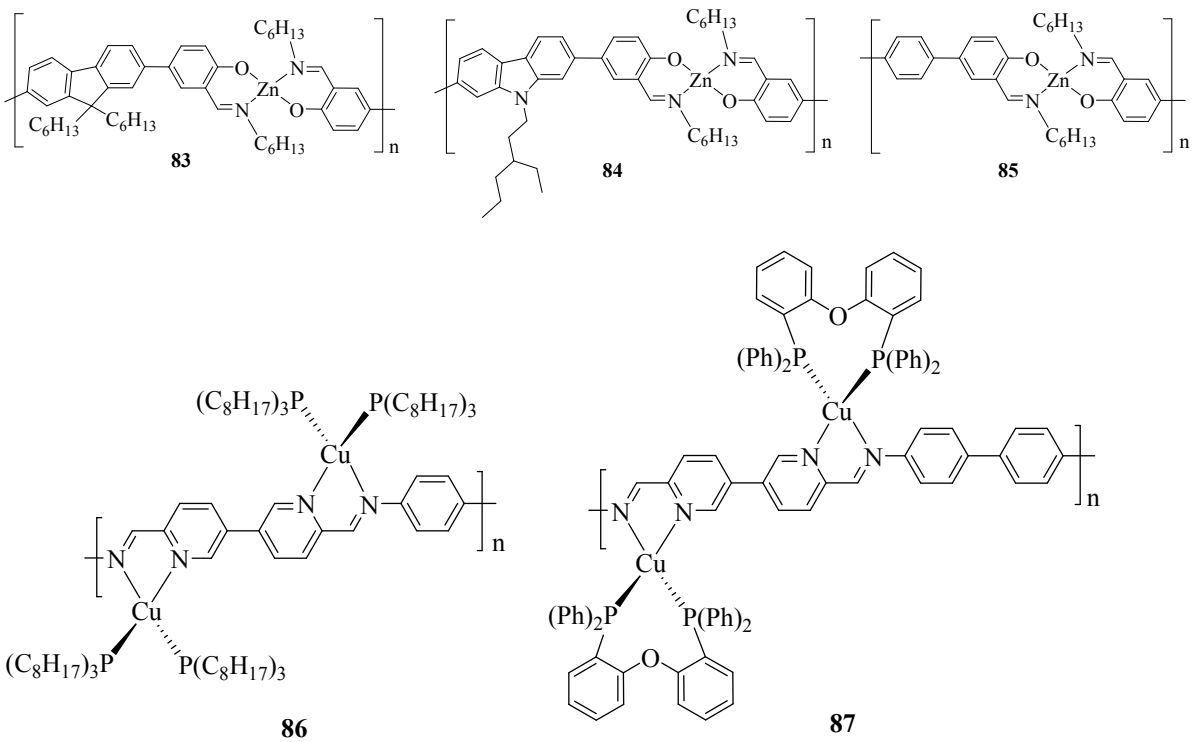

2.3 Multimetallic Schiff base assemblies

Taking advantages of the notion that the triplet state of a transition metal Schiff base lies at ~18,000 cm^{-1}, the metal chromophore can be exploited to act as the antenna for lanthanide-ion sensitization [68]. Such a strategy has been mostly used for sensitizing NIR emitting Ln(III) ions and the long-lived ^{3}MLCT states of d-block transition metals (e.g. Ru(II), Re(I), Os(II), Au(I), Pt(II) and Ir(III)) can be excited by visible light and transfer their energy efficiently onto the $4f^n$ manifolds, thus offering an effective pathway for energy migration within the heterometallic complexes. A series of 3d-4f bimetallic Schiff base complexes **88** was synthesized following the pathway shown in Fig. 6 [69,70]. It was shown that the relatively soft transition-metal ion Zn(II) is located in the inner N_2O_2 cavity and the Ln(III) ion in the outer O_4 cavity

of the compartmental Schiff base ligand. From the PL measurements, complexes **88** (Ln = Nd, Yb or Er) show emissions characteristic of the Ln(III) ion in the NIR region [69−71]. The NIR emissions of **88** originate from the absorption corresponding to the Zn(II) Schiff base complex. Thus, the Zn(II) Schiff base complex is capable of generating an antenna effect for Ln(III) ion. The effectiveness of this effect depends on the structure of the complex, the nature of the Ln(III) ion and the substituents on the Schiff base. The photophysics of the Schiff base complexes can be modified by varying the linkage between the two Schiff base units or the electronic properties of the substituents on the flanking phenyl groups [69].

Interestingly, it was found that the nuclearity of the 3d-4f metal Schiff base complexes can be easily manipulated by varying the ratio of the amounts of Zn(II) Schiff base complexes to $LnX_3 \cdot xH_2O$ and the nature of the anion X. Fig. 7 depicts some examples of the formation of mixed-metal Schiff base complexes of various metal nuclearity **89**–**92** [72,73]. The nuclearity of 3d-4f Schiff base complexes can also be increased by using different linking donor ligands (**93** and **94**) [74,75]. Detailed discussion of the structural and photophysical properties of these 3d-4f mixed-metal Schiff base complexes was reviewed before by Zhu et al.. Interested readers can refer to that review article [76].

New thermally stable Zn(II) dinuclear complexes based on bis(Schiff bases)

containing some pyridyl-functionalized ligands **95**−**98** were synthesized recently [77]. They possess various main group moieties (NPh_2, SO_2Ph, $POPh_2$ and $SiPh_3$) in the pyridyl ligands and emit fluorescence in both solution and PMMA-doped (PMMA = poly(methyl methacrylate) films. It was found that the PL emission intensity of these complexes can be enhanced by reducing the degree of molecular aggregation using the pyridyl-functionalized ligands. By virtue of the good charge-transporting/injection properties as well as the dendritic nature of the designed pyridyl ligands, the solution-processed OLEDs based on **95** can furnish the peak EQE of 1.46%, CE of 4.1 cd A^{-1} and PE of 3.8 lm W^{-1}.

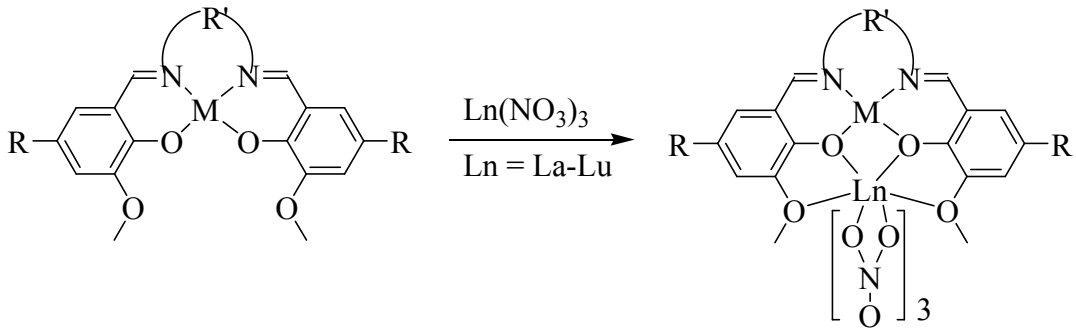

88

Fig. 6. Synthesis of some 3d-4f bimetallic Schiff base complexes **88**.

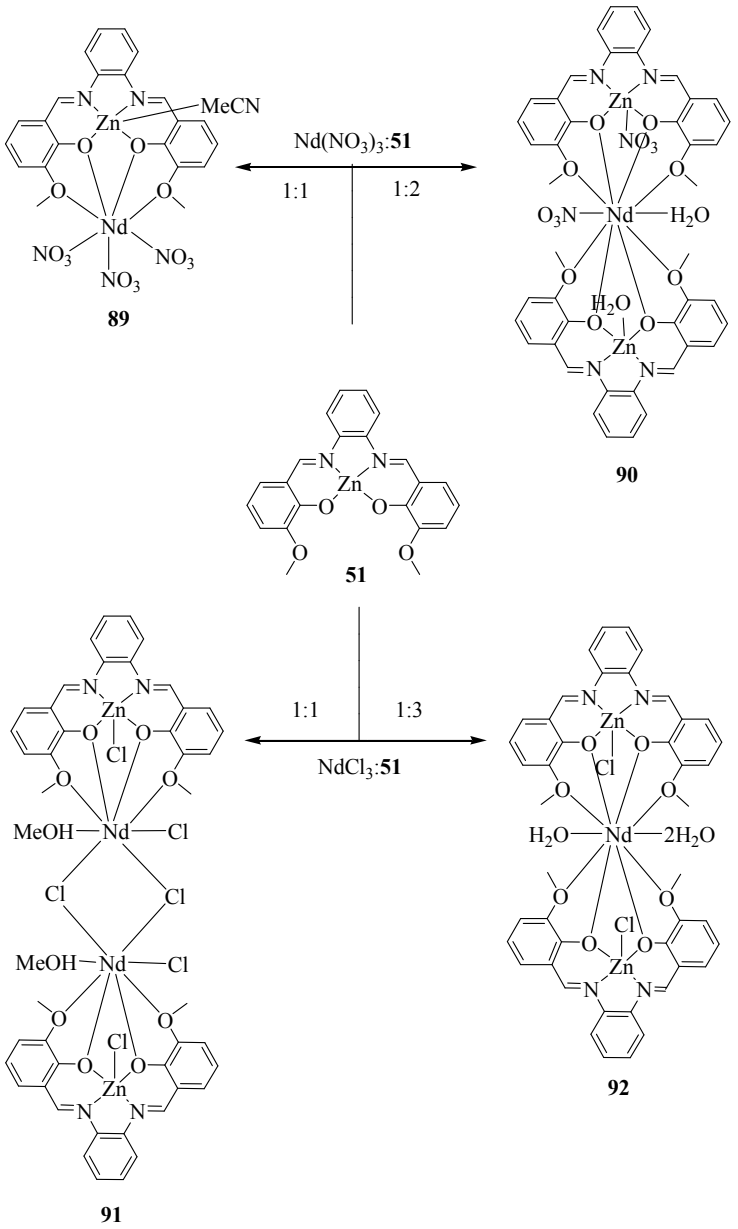

Fig. 7. Representative examples of the formation of mixed-metal Schiff base complexes of various metal nuclearity **89**–**92**.

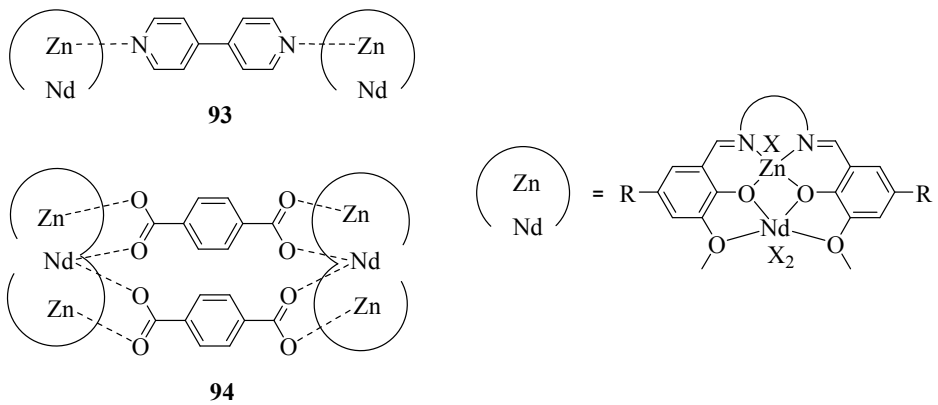

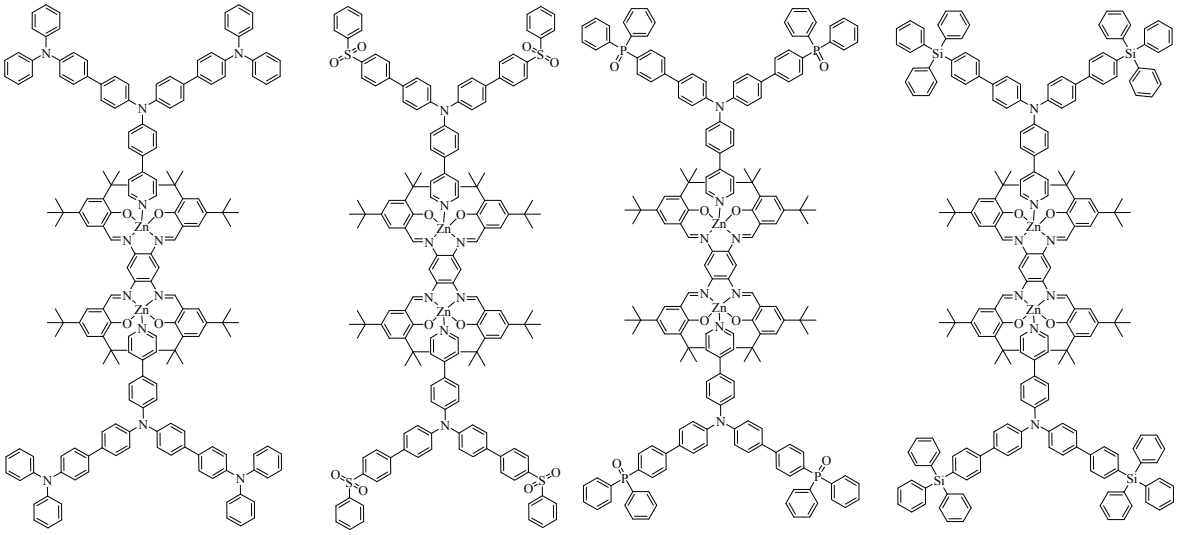

95 96 97 98

Table 1

Photophysical and thermal properties of **1**−**41**

Compound	λ_{max} [nm][a]	λ_{em} [nm][a]	Φ_{em} [%]	τ [μs]	HOMO/ LUMO [eV]	E_g [eV]	T_d [°C]	Ref
1	250, 314, 336, 417, 503[a]	550, 580[a]	19	3.5	-5.32/ -2.34	2.98	406	30,31
2	319, 345, 424	560	14	2.4	-5.34/ -2.48	2.86	315	31
3	250, 320[a], 340, 420, 500[a]	592	8.7	0.46	-5.32/ -2.32	3.00	369	30,31
4	246, 316, 339, 413, 432[a], 501[a]	541, 580[a]	18	3.4	-5.66/ -2.06	3.60	382	30,31
5	252, 317, 346, 427, 446[a], 520	556	23	2.88	-5.45/ -2.24	3.21	474	31
6	251, 316, 345, 423, 440[a], 514	551	26	3.81	-5.47/ -2.25	3.22	495	31
7	245, 320, 346, 429, 448[a], 529	568	13	2.32	-5.58/ -2.34	3.24	484	31
8	252, 319[a], 337, 409, 426[a], 493	548	8	1.68	-5.27/ -2.08	3.19	345	31
9	249, 306, 324, 394, 465	552	7	1.57	-5.26/ -2.21	3.05	379	31
10	242, 316, 352, 439, 458[a], 535	588	8	2.31	-5.23/ [b]	[b]	455	31

11	250, 312, 358, 376, 451, 504[a], 523	611	23	3.43	-5.37/ -2.89	2.48	415	31
12	255, 316, 361, 379, 460, 532	625	27	4.62	-5.40/ -2.88	2.52	339	31
13	250, 315, 357, 375, 453, 521	611	18	3.2	-5.34/ -2.96	2.38	411	31
14	250, 315, 357, 375, 453, 520	610	23	4.54	-5.35/ -2.93	2.42	396	31
15	248, 311, 360, 378, 455, 523	615	21	4.43	-5.39/ -3.00	2.39	414	31
16	244, 314, 361, 377, 467, 516[a], 546	649	7	2.87	-5.15/ -3.01	2.14	408	31
17	[b]	661	3.3	1.6	[b]	[b]	[b]	36
18	393, 453, 607	650, 776	8.6	1.97	-5.06/ -3.28	1.78	352	37
19	244, 336, 389, 407, 461, 491	531, 601, 654	4.4	1.82	-5.00/ -2.89	2.11	340	37
20	376, 396, 458, 491, 575	664	0.87	2.35	-5.42/ -3.50	1.92	350	37
21	263, 302, 327, 370, 388, 478, 526[a], 560	643	14	5.0	-5.37/ -2.93	2.41	[b]	38,42
22	259, 304[a], 329, 368, 387, 476, 519, 555	642	6	5.5	-5.36/ -2.96	2.40	[b]	42
23	261, 320, 367, 385, 470, 519[a], 546	632	6	3.5	-5.28/ -3.00	2.28	[b]	42
24	259, 322, 366, 384, 470, 515[a], 544	631	10	5.9	-5.23/ -2.98	2.25	[b]	42
25	253 , 316 , 353, 437	560, 602[a]	15	3.36	-5.18/ -2.63	2.55	380	39
26	261, 322, 351, 441	559, 603[a]	18	4.89	-5.09/ -2.56	2.53	330	39
27	258, 373, 389, 486, 561	650	12	2.60	-5.13/ -3.05	2.08	279	39
28	255, 311, 321, 359, 379, 454, 526	612, 673[a]	17	7.72	-5.10/ -2.89	2.21	388	39
29	262, 330, 373, 392, 497, 556	590[a], 649	11	2.85	-5.38/ -3.27	2.11	372	39
30	260, 319, 352,	568, 612[a]	15	3.94	-5.40/	2.52	336	39

	438				-2.88			
31	259, 337, 437	568	17	6.34	-5.19/ -2.68	2.51	401	39
32	248, 357, 425	557, 596[a]	16	8.39	-5.12/ -2.58	2.54	341	39
33	266, 357, 431	556	0.7	12.80	-5.23/ -2.72	2.51	341	39
34	287, 342, 432	565, 608[a]	20	5.37	-5.13/ -2.61	2.52	404	39
35	262, 319, 368, 386, 465, 534	624	20	6.3	-5.15/ -2.89	2.26	[b]	42
36	341, 472	[b]	[b]	[b]	-5.34/ -2.95	2.39	260	43
37	343, 487	527, 618	0.01	1.45	-5.49/ -3.12	2.37	295	43
38	267, 313, 386, 446	613	3.22	1.26	-5.47/ -2.93	2.54	272	43
39	337, 450, 511	593, 629	0.13	1.16	-5.36/ -3.31	2.05	281	43
40	337, 451, 497	565, 609	0.02	1.52	-5.43/ -3.37	2.06	284	43
41	299, 442	566, 606	7.92	1.88	-5.28/ -2.67	2.61	248	43

[a] shoulder peaks; [b] not reported.

Table 2

EL data of selected OLEDs

Compound	$\lambda_{em, EL}$ [nm]	Max. luminance [cd m^{-2}]	EQE [%]	CE [cd A^{-1}]	PE [lm W^{-1}]	Ref.
1	554	9,370		6.1		30,31
4	554	23,000		31		30,31
8	552	6,860		3.7		31
11	632	17,900		10.8		31
12	628	10,975		1.6		31
13	632	3,060		2.2		31
14	628	7,928		1.8		31
25	560	10,826	7.0	21	17	39
26	560	1,236	2.2	6.0	5.0	39
27	656	2,468	2.4	1.3	0.9	39
31	564	11,106	8.3	23	17	39
35	628	16,673	11.7	20.43	18.33	42
37	608	475	0.11	0.16	0.06	43
38	564	1,521	0.54	1.12	0.62	43
40	564	97	0.15	0.29	0.14	43
41	560	150	0.18	0.35	0.17	43

3. Light to electrical energy conversion in dye-sensitized solar cells

While OLEDs use electricity to produce light, another stream of current research focuses on the reverse of this process, i.e., using sunlight to produce electricity as in solar cell chemistry through a process called the photovoltaic effect [78,79]. Photovoltaic devices are able to convert (sun)light directly into electrical energy without any emissions of air pollutants and greenhouse gases. In an attempt to reduce the use of fossil fuels which are not eternal and heavily contribute to global warming, scientists are looking for other sustainable energy sources to serve our future energy needs. Of these, solar energy is promising because the Earth receives more energy from the Sun in one hour than is used by all of humanity in one year. Much research has gone into producing efficient organic solar cells. Solar energy is regarded as a renewable energy, and is environmentally-friendly, abundant and free. Therefore, direct photoconversion of solar energy by using photovoltaic technology is increasingly recognized worldwide as a viable hi-tech solution to the growing energy challenge [78,79]. Although inorganic materials have so far dominated the field, organic materials as photovoltaics are also attracting a lot of research attention because of their favorable environmental and inexpensive features. Dye-sensitized solar cells (DSSCs) represent one of the most promising types of organic solar cells to date [80].

A classical DSSC consists of two glass plates coated with a transparent conductive oxide layer. The working electrode is covered with a film of a dye-sensitized substance and the counter electrode is coated with a catalyst. Both plates are sandwiched together with the gap between them filled by an electrolyte containing a redox mediator. Light absorption is carried out by dye molecules (organic or metal-organic) in which the absorbed photons cause dye photoexcitation to release an electron rapidly to the semiconductor. The injected electrons then hop through the colloidal TiO_2 particles to reach the collector. Following this, the electron passes through an outer circuit to reach the other transparent conductive oxide layer at the counter electrode, ultimately doing electrical work for the user. Finally, the electron is then transferred to the electrolyte where it reduces the oxidant and the reduced form reduces the excited dye to the ground state and completes the circuit [81]. In particular, metal Schiff base complexes were found to play many important roles in the advancement of DSSCs in some recent research activities. The following illustrates some recent examples.

Indeed, metal Schiff base complexes can serve as the photosensitizer, electrolyte or redox mediator in DSSCs. Investigations have suggested that conjugated poly(Schiff bases) as new semiconducting materials have good stability, electroactivity and electrical conductivity [82]. The presence of conjugated bonds

triggers electron delocalization along the polymer chain and potentially leads to high charge carrier mobility. It was demonstrated that conductive polymers based on [M(salen)] (M = Ni, Pd, Pt) are promising materials for use as electrodes for photoelectrochemical energy conversion. The [M(salen)] complexes can specifically adsorb onto the electrode (substrate) to produce stacks with individual fragments bound by D-A and intermolecular interactions. When the electrode potential was shifted to the anodic region, the stacks were cross-linked due to the formation of C−C bonds between the individual monomers (Fig. 8) [83]. The electrochemical polymerization of poly-$[M(salen)]_n$ film was carried out on the surfaces of working glassy carbon electrodes from the solution of 1 M [M(salen)] monomer in CH_3CN. When [M(salen)] is used as a photosensitizer in the Gratzel-type of cell, rapid electron transfer from the excited state of [M(salen)] to the band zone of TiO_2 takes place instead of a reaction with O_2.

Metalloporphyrins and their analogues represent attractive candidates for use in photovoltaics [84−86]. They show intense absorption with high molar extinction coefficients in both the blue (Soret band) and red (Q-band) regions. Their photo- and electrochemistry can be easily tuned by peripheral functionalization and varying the metal center. It has been shown that push-pull metalloporphyrin derivatives can be successfully applied in DSSCs. A series of metalloporphyrins bearing the Schiff base

imine linkage **99**−**102** were reported in the literature for DSSC applications [87−90]. Complex **99** consists of the porphyrin donor group with 3,4,5-trimethyloxybenzaldehyde and acceptor/anchoring unit (carboxyl group) connected to the imine -C_6H_4-N=CH- moiety. A control dye without such an imine group was also made for comparison in order to study the effect of the Schiff base entity on the DSSC cell performance. The absorption spectrum of **99** shows a broader and stronger band than the control dye [87,88]. The absorption bands of **99** (ca. 431, 564 and 606 nm) are red-shifted from those of the control (ca. 423, 559 and 600 nm). The incorporation of the Schiff base functionality at the *meso* position shifted the energy level of oxidation potential (E_{ox}) to the positive relative to the reference dye, leading to a decreased HOMO-LUMO gap. It is inspiring to see that photosensitizer **99** shows a better DSSC cell performance than the control dye and the device parameters are impressive at the power conversion efficiency (PCE) of 1.75% with short-circuit current density (J_{sc}) of 5.5 mA cm^{-2}, open-circuit voltage (V_{oc}) of 0.65 V and fill factor (FF) of 0.65. The control dye only showed a PCE of 1.06% under the same conditions. Another complex **100** was also studied preliminarily but there is no mention of the DSSC data [89]. Moreover, the two Schiff base-containing metalloporphyrins **101** and **102** were employed to modify TiO_2 electrodes for supramolecular solar cells using the metal-ligand axial coordination assembling

strategy [90]. These two assemblies are based on the two porphyrins appended isonicotinic acid ligands and can be adsorbed on the semiconducting TiO_2 electrode surfaces by using the carboxylic groups of isonicotinic acid ligands. The DSSC cell performances were evaluated under irradiance of 100 mW cm^{-2} AM 1.5G sunlight. It was found that dye **102** outperformed **101** in the photovoltaic behavior by over 20% and the PCE of the device based on **102** is 0.21% with J_{sc} = 1.20 mA cm^{-2}, V_{oc} = 0.27 V and FF = 0.65.

In order to enhance the V_{oc} of DSSC, a more positive redox potential of the redox mediator is critical. While the classic redox mediator in DSSCs is the I_3^-/I^- redox couple, a new cobalt(II) Schiff base complex **103** was prepared and used as an efficient redox mediator system in DSSCs [91]. The Co(II)-salen Schiff base complex **104** was also studied for comparison. Due to the non-reversible reaction of **104**, the DSSC cell fabricated with **104** did not show any photocurrent. As compared to the conventional redox mediator $[Co(bipy)_3]^{2+}$, the V_{oc} in the device was improved for compound **103** but the J_{sc}, FF and PCE are still lower than those of $[Co(bipy)_3]^{2+}$. It was shown that complex **103** has a lower symmetry and that the two free OH groups on the ligands can increase the charge transfer resistance between **103** and the platinum surface at the counter electrode, which would decrease the FF and PCE of the cell. The OH groups can increase the negative charge distribution on the complex

and create a resistance between the cobalt center and platinum surface by a charge repulsion phenomenon. Next, free OH groups can adsorb on the uncoated TiO_2 surface by the formation of hydrogen bonding to oxygen atoms or coordinate bonding with Ti atoms. This would decrease the PCE of the cell by increasing the recombination reactions between the uncoated TiO_2 surface and the redox mediator.

The nickel(II) Schiff base complex **105** was also reported which can be applied as a suitable electrolyte in DSSC application [92]. Because of its high reductive activity and conductivity, a higher J_{sc} and incident photon-to-current efficiency (IPCE) was obtained. In such study, the composition of the electrolyte was also optimized in order to maximize the photocurrent. It was shown that the best ionic conductivity of 0.523 S m^{-1} was achieved if the electrolyte consists of complex **105** (0.1 mol L^{-1}) and I_2 (0.05 mol L^{-1}), resulting in the PCE of 7.75%. This offers a new venture toward enhancing the performance of DSSC.

Substituted Schiff base complexes of Zn(II) **106**−**108** were developed and their use as the co-sensitizer in photoanodes for the fabrication of co-sensitized DSSCs was examined [93]. These complexes are all luminescent and their PL properties were compared to their group 12 congeners (Cd(II) and Hg(II) complexes). The Zn(II) complexes show the highest Φ_{em} among the series which is due to the structure-induced luminescence phenomenon. Complexes **106**−**108** display absorption peaks in

the region of 300-450 nm, which can compensate for that of the classical dye N719 in the low-wavelength region of the visible spectrum and offset competitive visible-light absorption of I_3^-. Upon co-sensitization, the performances of all the devices were improved. The J_{sc}, V_{oc} and PCE were increased following the order of **108**/N719 > **107**/N719 > **106**/N719 > N719. Among these, the **108**/N719 cell gave the highest J_{sc} of 16.59 mA cm^{-2} and PCE of 6.94%, which is 36% higher than those of the devices from N719 only (5.11%). The results are consistent with the data obtained by electrochemical impedance spectroscopy (EIS). From the Nyquist plots of the cells, the radii of the large semi-circle located in the middle-frequency region decrease in the order of **108**/N719 < **107**/N719 < **106**/N719 < N719, which shows a decrease of the electron transfer impedance and an increase of charge transfer rate at this interface after co-sensitization. Moreover, based on the dark-current measurement of DSSCs, the increase of the onset potential and the reduction of the dark current indicated that **106**−**108** can suppress the electron back reaction with I_3^- in the electrolyte. In terms of structural reasons, when the electron-donating power of the substituent groups in aniline increases in the order of OMe > Me > ^{i}Pr, the PCE would increase. For **108**, the best PCE can be explained by the red-shift of the absorption features and the largest molar extinction coefficient in the presence of OMe group as well as the smallest dihedral angle between the pyridine ring and the phenyl ring (almost co-

planar) in this complex.

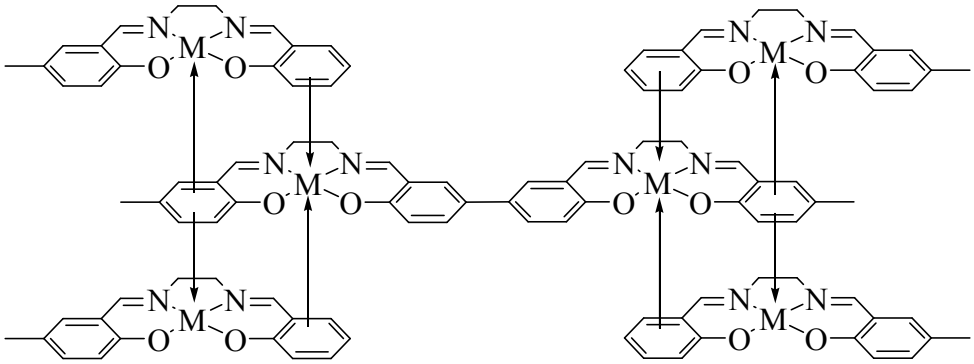

Fig. 8. Structure of poly-[M(salen)] polymers (M = Ni, Pd, Pt).

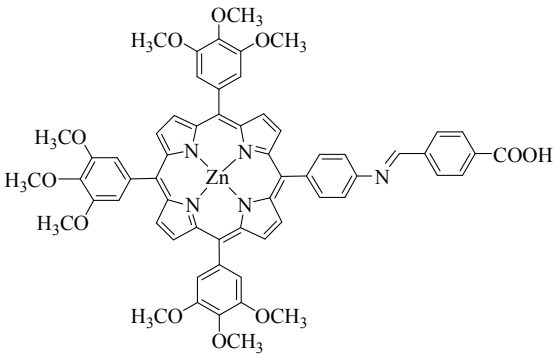

99

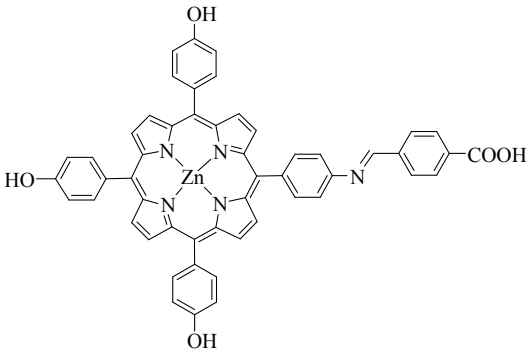

100

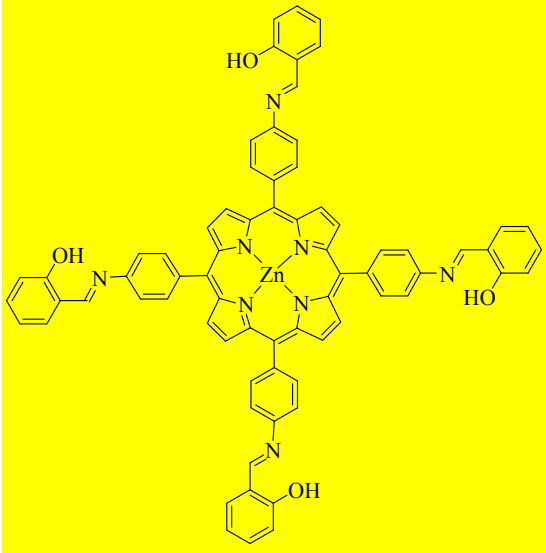

101

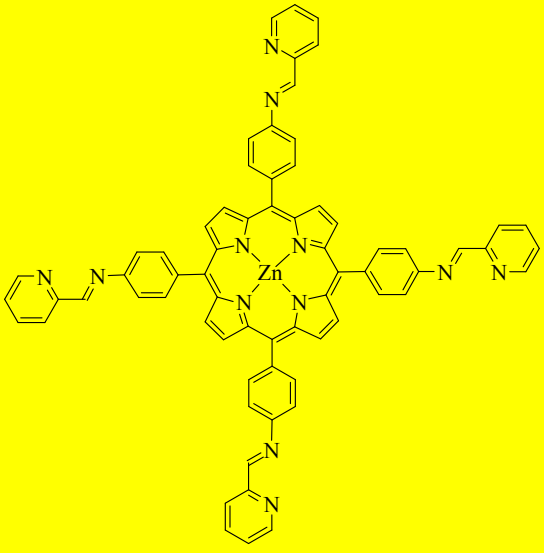

102

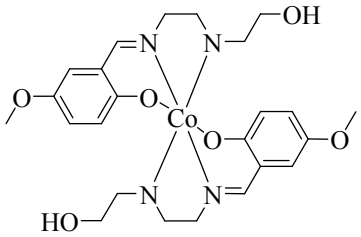

103

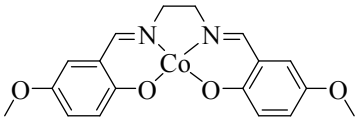

104

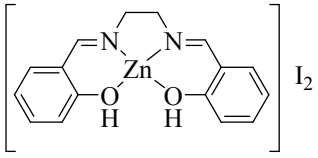

105

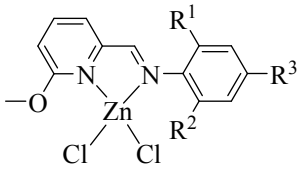

$R^1 = R^2 = {}^iPr$, $R^3 = H$ **106**
$R^1 = R^2 = H$, $R^3 = Me$ **107**
$R^1 = OMe$, $R^2 = R^3 = H$ **108**

4. Other energy-related applications

4.1 Conductive metallopolymers and their relevance in thermoelectric applications

Recently, thermoelectric (TE) materials have received a great deal of attention because of their unique ability to convert heat into electricity without any moving parts or bulk fluids and vice versa [94−97]. The energy conversion efficiency of TE materials is determined by their TE figure of merit, $ZT = S^2\sigma T/K$, where S is the Seebeck coefficient (thermopower), σ is the electrical conductivity, K is the thermal conductivity, and T is the absolute temperature. Inorganic materials, such as Bi_2Te_3 [98], PbTe-$AgSbTe_2$ (ZT reaching 2.1 near 800 K) [99] and SnSe [100], have been extensively studied for several years because of their relatively high ZT value. However, these materials also possess clear disadvantages such as poor processability, toxicity, brittleness and high cost, which have impeded their widespread use as energy materials. In contrast, polymeric materials possess unique

features that are useful in applications as TE materials such as low-cost, ease of synthesis, solution processability over a wide range of parameter values and an intrinsic low thermal conductivity. Following the initial discovery of conducting polymers in the late 1970s, polymers such as polyaniline, polythiophene, polyacetylene, polypyrrole and their derivatives, have received increasing attention as prospective TE materials [94−97]. If the TE power factor (PF = $S^2\sigma$) of conductive polymers could be substantially improved, these materials could be used in many TE applications. More recently, a new class of polymers based on metal-coordinated tetrathiolate has been shown to possess very promising *p*-type and *n*-type TE properties with their ZT over 0.015 at 400 K and 0.2 at 440 K, respectively. The TE properties of poly-[A_x(A-ett)]s (A = Ni, Cu; ett = 1,1,2,2-ethenetetrathiolate) have been well studied [101]. These encouraging TE properties in metalated polymers open up a new direction for the development of high ZT organic materials. In this context, conducting metallopolymers with good σ values hold great promise in the development of new TE materials. Previously, a large series of conducting transition metal Schiff base polymers is known in the literature. Schiff base polymers **109**−**111** were studied for their electrical properties and their S values were measured from the TE voltage as determined by a potentiometric method [102,103]. The positive S value indicates the predominance of holes as the majority charge carriers (i.e. a *p*-type

semiconductor). For **110**, the conductivity trend follows the order Cu(II) > Ni(II) > Co(II). In the case of **110** (M = Cu(II)), the S value ranges around 1.1−1.3 mV K^{-1} (1.15 mV K^{-1} at 300 K) and a hopping type of mechanism for the charge carriers was proposed. As mentioned above, high electrical conductivity is one of the key factors in designing good TE polymers and it would be promising to survey some conductive metallopolymers of the Schiff base ligands here for the future development of new TE metallopolymers. For instance, a series of conducting Schiff base-containing metallopolymers **112**−**123** was reported [104−110] and the nature of electrical conductivity in some of these systems was elucidated in detail. The effect of redox matching has been well demonstrated. For the redox-matched system in **112**, the matching of the metal and polymer backbone centered redox potentials leads to a conductivity enhancement beyond a simple additive combination. However, the lack of redox matching in **113** results in a relatively low conductivity [104]. The metal-induced conductivity enhancement effect was demonstrated in conducting metallopolymers of a Schiff-base ligand **115** relative to its metal-free congener [106]. The maximum conductivities of **113** and **115** are 40 [104] and 83.4 S cm^{-1} [106], respectively. The charge injection and transport properties in **119**−**122** were also examined. For the cobalt-containing polymers **119** and **121**, both the metal centers and π-conjugated organic backbone work cooperatively as hopping stations for

migrating holes, while the reduced polymer utilizes less-efficient self-exchange between Co(II) and Co(I) centers for electron transport [108]. Although there is no thermoelectric data available yet for these metallopolymers, there is a good prospect of using these conductive materials for such applications in the future.

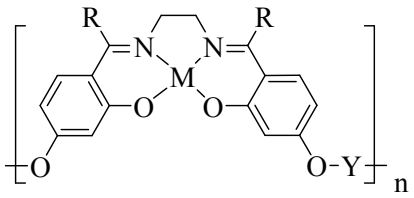

M = Ni^{2+}, Cu^{2+}
R = H, CH_3, C_6H_5

Y =

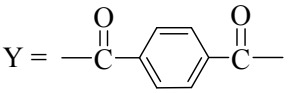

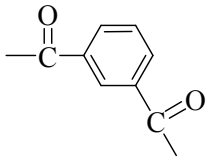

109

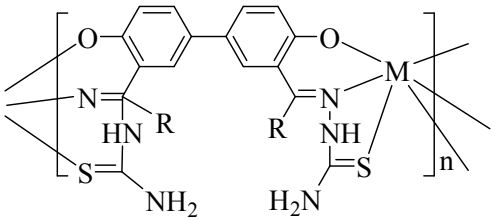

M = Cu^{2+}, Ni^{2+}, Co^{2+}

110 R = CH_3

111 R = C_2H_5

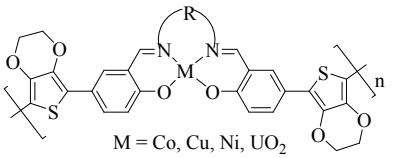

M = Co, Cu, Ni, UO_2

R=

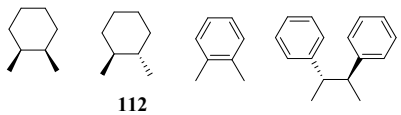

112

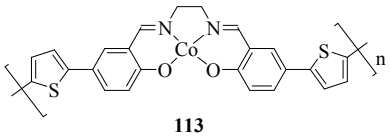

113

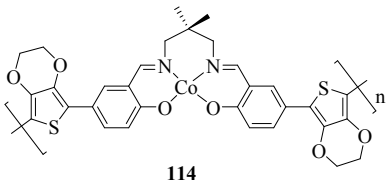

114

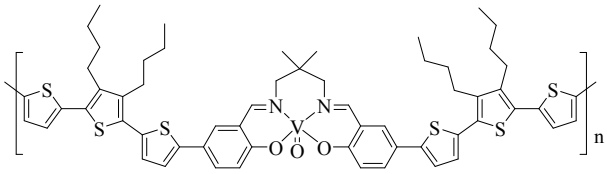

115

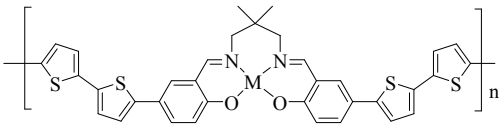

116: M = Ga-Cl
117: M = Ga^{+}

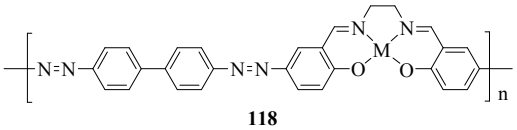

118

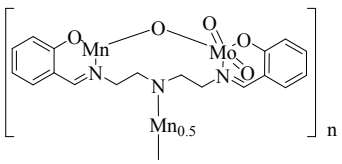

123

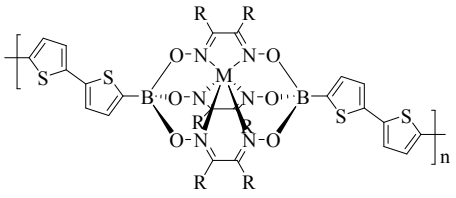

119 (M = Co)
120 (M = Fe)

R =

121 (M = Co)
122 (M = Fe)

R R =

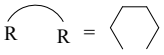

4.2 Energy storage materials in batteries and supercapacitors

With the rapid development of the global economy, the depletion of fossil fuels and increasing environmental pollution, there is an upsurge of interest in the search for efficient, clean and sustainable sources of energy (e.g. sun and wind), as well as new technologies associated with energy conversion and storage. Since the sun does not shine during the night, and wind does not blow on demand, energy storage systems are playing a larger part in our lives. At this forefront, electrical energy storage systems such as batteries and electrochemical capacitors (or supercapacitors) are gaining much attention [111−114].

The search for new battery materials and chemistry with high-power and high density energy storage is an important topic for tomorrow's energy storage needs [115−117]. Development of high-performance organic batteries is one of the key technologies necessary for an extensive market of energy storage systems [118−120]. Rechargeable secondary lithium ion batteries are currently the systems of choice, offering high energy density, flexible and lightweight design and longer lifespan than comparable battery technologies [115−117]. As a rising star in electrochemical energy-storage systems, new-generation organic batteries are expected to complement or replace traditional batteries in certain applications. Organic batteries are considered attractive alternatives to conventional inorganic energy-storage analogues for applications that demand low-cost, low-temperature fabrication, solution-phase device

processing and mechanical flexibility [118−120]. As the core element of an organic battery, electroactive organic polymers with high performance and excellent redox stability are necessary for practical applications. To date, many redox-active organic polymers have been developed, and among these, radical polymers have become the benchmark for this field [119−121]. Yet, the way to promote the multi-electron redox reactions in battery systems remains a big challenge for scientists. Recently, electroactive polymeric (linear or hyperbranched) and oligomeric organic Schiff bases have shown promising performance as negative electrode (anode) in sodium ion batteries [122−124]. Electrochemical activity can be expected from the existence of the Schiff base functionality (viz. C=N double bond). Although the azomethine group is more easily reducible than the corresponding carbonyl group of the parent compound, the redox voltage can be tuned just by lengthening the conjugation chain, formation of intramolecular hydrogen bonds or introduction of D or A groups in the aromatic units. Moreover, a series of high nitrogen-content carbon nanosheets formed through the Schiff-base reaction in a molten salt medium was also used as anode materials in lithium ion batteries [125−127]. Their large surface area, high nitrogen content and two-dimensional structure are not only favorable for the fast and steady transfer of electrons and ions, but also offer more active sites for lithium storage, thus resulting in high specific capacity and good rate performance. Moreover, these carbon

nanosheet materials with high nitrogen content offer great potential in other energy applications such as supercapacitors. Supercapacitors, which bridge the gap between conventional dielectric capacitors and batteries in terms of both energy and power densities, are currently attracting intensive attention in the scientific community because they can provide energy density higher by orders of magnitude than dielectric capacitors, and greater power density and longer cycling ability than batteries [111−114]. Accordingly, supercapacitors have an important role in complementing or replacing batteries in electrical energy storage and harvesting applications, when high power delivery or uptake is needed.

Peripheral covalent modification of inorganic and organometallic compounds by post-functionalization is a versatile synthetic method nowadays to develop new functional molecules [128]. A post-functionalized metalated covalent organic framework **124** containing tetramethyl-1-piperidinyloxy (TEMPO) moieties was prepared. TEMPO is a typical organic radical that not only exhibits all the unique properties of radicals but also possesses redox ability for energy storage by reversibly switching between the oxidation states of the neutral radical and oxoammonium cation. As a result, compound **124** shows rapid and reversible redox reactions, giving rise to high capacitance, high rate and robust cycle stability [129].

An investigation into the chemical reduction of early transition metal Schiff base

complexes leads to a molecular battery system in which it provides a good way of storing and releasing electrons based on the reversible formation and cleavage of C−C bonds, which can be coupled to the change of the oxidation state of the metal. The C−C bond actually functions as a two-electron reservoir without being involved in the chemical reactivity. The reduction of titanium(III) complex **125** and vanadium(III) complex **126** by sodium metal resulted in the reductive coupling of imino groups in the Schiff base ligands and then the formation of C−C bonded dimers (**127** and **128**, respectively), which can release electrons on subsequent cleavage of the C−C bond. Further reduction of **127** and **128** by sodium metal led to the formation of complexes **129** and **130**, respectively (Fig. 9). In this study, the authors have been able to explore the reactivity of the reduced species of the titanium and vanadium compounds [130]. In these reactions, the electrons stored at the C−C bond and in the metal atom can be selectively used, either separately or altogether, in the reduction of O_2, quinones and other substrates. An extended Hückel analysis showed that the reduction of Ti(III) and V(III) salphen complexes takes place with the electron density stored at the carbon centers involved in the C−C bridges across the two salphen units. Such calculations also reveal that the first step in the transfer of the electrons stored at the C−C bonds occurs with the oxidation of the metal, followed by an electron removal from nitrogen, and then the cleavage of the C−C bridge, which is never involved directly as

a reactive site.

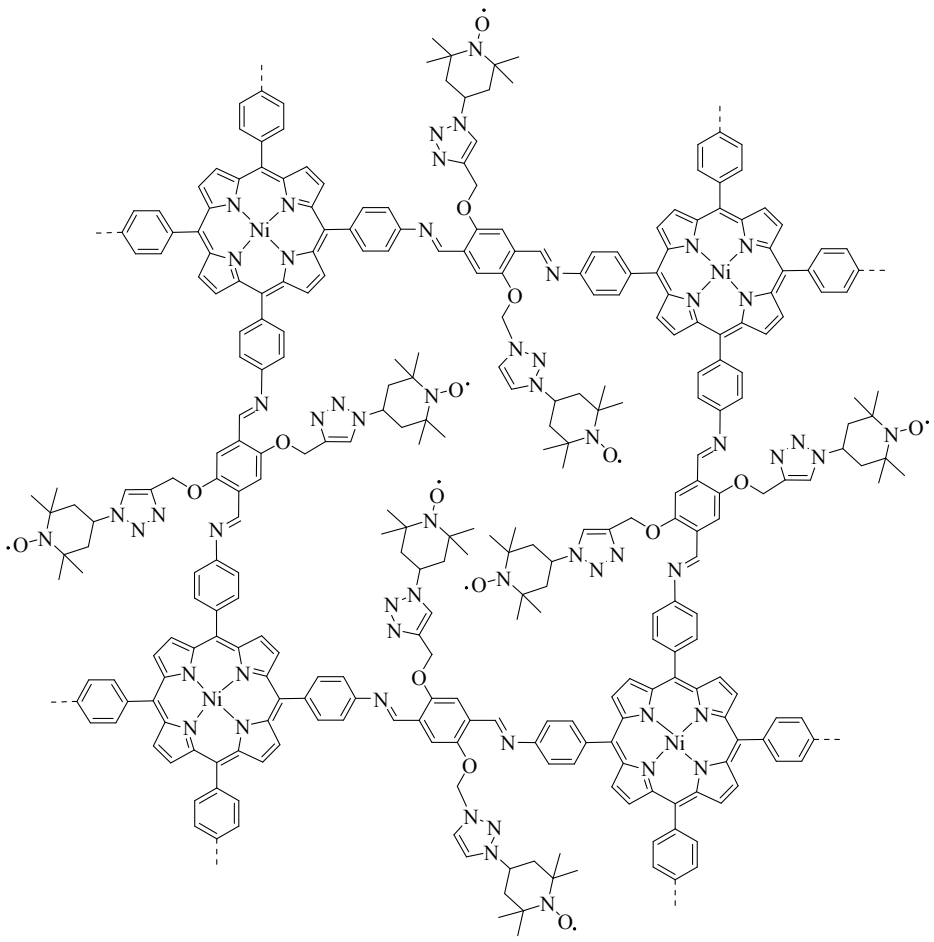

124

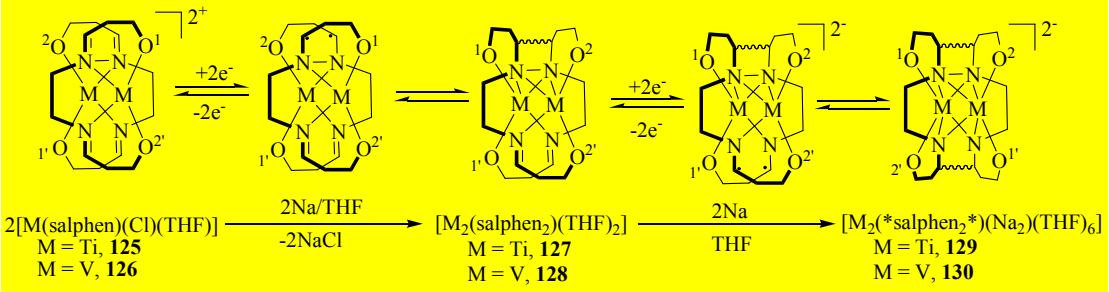

Fig. 9. A molecular battery system based on carbon-carbon bond formation and cleavage in titanium and vanadium Schiff base complexes. *Salphen$_2$* is a dinucleating, octadentate, octaanionic ligand.

5. Concluding remarks and future perspectives

Molecular semiconductors are attracting much current attention in the scientific community and one key focus is shifted toward utilizing them in energy research in recent years. The transformations of light into electricity and electricity into light represent two complementary topics that are highly relevant to the solution of the worldwide energy problem. Inorganic chemistry is particularly vital to such development. Coordination and organometallic compounds have been widely investigated in these energy-generating (solar cell) and energy-saving (OLED) applications. These energy conversion materials are useful for the efficient production, transformation and utilization of the two energy forms. In particular, metal Schiff base complexes are attractive in the context of practical applications because of the ease of synthesis of the Schiff base ligands, high coordination affinity toward a variety of metal ions, robust chemical nature and the simplicity of scaling up for mass production. It is well-known that salicylaldiminato Schiff bases readily form stable transition metal complexes by complexation with metal ions such as Cu(II), Ni(II), Co(II), Zn(II), Mn(II), Fe(II), Pt(II), etc.. Structural diversity of the Schiff base ligand allows facile tailoring of the properties of this class of metalated molecules. In the past few decades, impressive progress has been made in this research frontier and

this article provides a detailed survey of the syntheses, photophysics and optoelectronic applications of these metallo(salen)s and related molecules. The chemical and physical properties of these photofunctional materials can be fine-tuned simply by varying their molecular structures via chemical modifications of their metal and ligand chromophores to develop the best materials for a particular function. While the use of these metal Schiff base complexes in the OLED field are becoming more mature at this stage, it would be anticipated that new emerging applications can also be realized with metallo(salen)s possessing multifunctional utilities. The area will continue to expand with the discovery of more functional materials of the metal Schiff bases. Molecular control of the materials properties and rational design of new generation materials through innovative chemical synthesis will certainly lead to a prosperous future of this field for many years to come. Especially, Pt(II) complexes are advantageous over d^6 octahedral metal complexes (e.g. Ru(II) and Ir(III)) for the OLED applications under certain circumstances because tetradentate ligand scaffolds in Pt(II) Schiff base complexes are relatively easy to construct and modify [131]. The potential of exploiting these metal Schiff base complexes in WOLEDs as next generation illumination sources and backlights for LCDs is also worthy of intensive investigation.

To draw a simple conclusion here, metal Schiff base chemistry can and will

make important contribution to the global energy problem. A large number of scientists have reported on the different types of metal Schiff base complexes that can function as molecular materials for various energy conversion processes. We look forward to these continuing developments with much optimism. In several cases, there are also examples of molecules that can even serve as multifunctional materials and can be applied both in energy conversion (e.g. light ↔ electrical and thermal → electrical) and energy storage devices. Therefore, many exciting future challenges exist for both exploratory and applications-oriented research based on these metal Schiff base molecules.

Acknowledgements

J. Zhang and L. Xu are co-first authors and they contributed equally to this article. We are grateful to the financial support from the National Natural Science Foundation of China (project numbers 51373145 and 21501128), Hong Kong Research Grants Council (PolyU 12338416), Areas of Excellence Scheme, University Grants Committee of HKSAR (AoE/P-03/08) and the Hong Kong Polytechnic University (1-ZE1C).

References

[1] J.A. Turner, Science 285 (1999) 687−689.

[2] R. Eisengberg, D.G. Nocera, Inorg. Chem. 44 (2005) 6799−6801.

[3] E. Baranoff, J.-H. Yum, M. Grätzel, M.K. Nazeeruddin, J. Organomet. Chem. 694 (2009) 2661−2670.

[4] M.K. Nazeeruddin, M. Grätzel, Struct. Bond. 123 (2007) 113−175.

[5] G.R. Whittell, M.D. Hager, U.S. Schubert, I. Manners, Nat. Mater. 10 (2011) 176−188.

[6] A. Wild, A. Winter, F. Schlutter, U.S. Schubert, Chem. Soc. Rev. 40 (2011) 1459−1511.

[7] R.P. Kingsborough, T.M. Swager, Prog. Inorg. Chem. 48 (1999) 123−231.

[8] K.A. Green, M.P. Cifuentes, M. Samoc, M.G. Humphrey, Coord. Chem. Rev. 255 (2011) 2530−2541.

[9] C.-L. Ho, W.-Y. Wong, Coord. Chem. Rev. 255 (2011) 2469−2502.

[10] C.-L. Ho, Z.-Q. Yu, W.-Y. Wong, Chem. Soc. Rev. 45 (2016) 5264−5295.

[11] T. Katsuki, Coord. Chem. Rev. 140 (1995) 189−214.

[12] K. Li, G.S.M. Tong, Q. Wan, G. Cheng, W.-Y. Tong, W.-H. Ang, W.-L. Kwong, C.-M. Che, Chem. Sci. 7 (2016) 1653−1673.

[13] A.C.W. Leung, M.J. MacLachlan, J. Inorg. Organomet. Polym. Mater. 17 (2007) 57−89.

[14] A.W. Jeevadason, K.K. Murugavel, M.A. Neelakantan, Renew. Sustain. Energy Rev. 36 (2014) 220−227.

[15] P.G. Lacroix, Eur. J. Inorg. Chem. 2 (2001) 339−348.

[16] W. Zhang, N.H. Lee, E.N. Jacobsen, J. Am. Chem. Soc. 116 (1994) 425−426.

[17] M. Tokunaga, J.F. Larrow, F. Kakiuchi, E.N. Jacobsen, J. Org. Chem. 63 (1998) 5252−5254.

[18] M.A. Baldo, M.E. Thompson, S.R. Forrest, Pure Appl. Chem. 71 (1999) 2095−2106.

[19] X. Yang, G. Zhou, W.-Y. Wong, Chem. Soc. Rev. 44 (2015) 8484−8575.

[20] Y. Chi, P.T. Chou, Chem. Soc. Rev. 39 (2010) 638−655.

[21] W.-Y. Wong, C.-L. Ho, J. Mater. Chem. 19 (2009) 4457−4482.

[22] P.-T. Chou, Y. Chi, Eur. J. Inorg. Chem. (2006) 3319−3332.

[23] J.A.G. Williams, S. Develay, D.L. Rochester, L. Murphy, Coord. Chem. Rev. 252 (2008) 2596−2611.

[24] W.-Y. Wong, C.-L. Ho, Coord. Chem. Rev. 253 (2009) 1709−1758.

[25] Q.S. Zhang, Q.G. Zhou, Y.X. Cheng, L.X. Wang, D.G. Ma, X.B. Jing, F.S. Wang, Adv. Funct. Mater. 16 (2006) 1203−1208.

[26] F. Wu, J. Li, H. Tong, Z. Li, C. Adachi, A. Langlois, P.D. Harvey, L. Liu, W.-Y. Wong, W.-K. Wong, X. Zhu, J. Mater. Chem. C 3 (2015) 138−146.

[27] M.A. Baldo, D.F. O'Brien, Y. You, A. Shoustikov, S. Sibley, M.E. Thompson, S.R. Forrest, Nature 395 (1998) 151−154.

[28] M.A. Baldo, S. Lamansky, P.E. Burrows, M.E. Thompson, S.R. Forrest, Appl. Phys. Lett. 75 (1999) 4−6.

[29] S. Lamansky, P. Djurovich, D. Murphy, F. Abdel-Razzaq, H.-E. Lee, C. Adachi, P.E. Burrows, S.R. Forrest, M.E. Thompson, J. Am. Chem. Soc. 123 (2001) 4304−4312.

[30] C.M. Che, S.C. Chan, H.F. Xiang, M.C.W. Chan, Y. Liu, Y. Wang, Chem. Commun. (2004) 1484−1485.

[31] C.M. Che, C.C. Kwok, S.W. Lai, A.F. Rausch, W.J. Finkenzeller, N.Y. Zhu, H. Yersin, Chem. Eur. J. 16 (2010) 233−247.

[32] H. Yersin, Top Curr. Chem. 191 (1997) 1−40.

[33] H. Yersin, D. Donges, Top. Curr. Chem. 214 (2001) 81−186.

[34] H. Yersin, W. Humbs, J. Strasser, Coord. Chem. Rev. 159 (1997) 325−358.

[35] H. Yersin, W. Humbs, J. Strasser, Top. Curr. Chem. 191 (1997) 153−249.

[36] G.S.M. Tong, P.K. Chow, W.P. To, W.M. Kwok, C.M. Che, Chem. Eur. J. 20 (2014) 6433−6443.

[37] J. Zhang, G.L. Dai, F.S. Wu, D. Li, D.C. Gao, H.W. Jin, S. Chen, X.J. Zhu, C.X. Huang, D.M. Han, J Photochem. Photobio. A 316 (2016) 12−18.

[38] B. Blondel, F. Delarue, M. Lopes, S. Ladeira-Mallet, F. Alary, C. Renaud, I. Sasaki, Synth. Met. 227 (2017) 106−116.

[39] J. Zhang, F.C. Zhao, X.J. Zhu, W.K. Wong, D.G. Ma, W.Y. Wong, J. Mater. Chem. 22 (2012) 16448−16457.

[40] K. Li, X.G. Guan, C.W. Ma, W. Lu, Y. Chen, C.M. Che, Chem. Commun. 47 (2011) 9075−9077.

[41] G. Zhou, Q. Wang, X. Wang, C.-L. Ho, W.-Y. Wong, D. Ma, L. Wang, Z. Lin, J. Mater. Chem. 20 (2010) 7472−7484.

[42] L. Zhou, C.L. Kwong, C.C. Kwok, G. Cheng, H.J. Zhang, C.M. Che, Chem. Asian J. 9 (2014) 2984−2994.

[43] J. Zhang, X.J. Zhu, A.G. Zhong, W.P. Jia, F.S. Wu, D. Li, H.B. Tong, C.L. Wu, W.Y. Tang, P. Zhang, L. Wang, D.M. Han, Org. Electron. 42 (2017) 153−162.

[44] H.F. Xiang, S.C. Chan, K.K.Y. Wu, C.M. Che, P.T. Lai, Chem. Commun. (2005) 1408−1410.

[45] T. Sano, Y. Nishio, Y. Hamada, H. Takahashi, T. Usuki, K. Shibata, J. Mater. Chem. 10 (2000) 157−161.

[46] G. Yu, Y.Q. Liu, Y.R. Song, X. Wu, D.B. Zhu, Synth. Met. 117 (2001) 211−214.

[47] A.A. Vashchenko, L.S. Lepnev, A.G. Vitukhnovskii, O.V. Kotova, S.V. Eliseeva, N.P. Kuzmina, Opt. Spectrosc. 108 (2010) 463−465.

[48] L.S. Lepnev, A.A. Vaschenko, A.G. Vitukhnovsky, S.V. Eliseeva, O.V. Kotova, N.P. Kuzmina, J. Russ. Laser Res. 29 (2008) 497−503.

[49] L. Lepnev, A. Vaschenko, A. Vitukhnovsky, S. Eliseeva, O. Kotova, N. Kuzmina, Synth. Met. 159 (2009) 625−631.

[50] Z.X. Gao, Y.Y. Hao, J.F. Lei, C. Ma, B.S. Xu, Optoelectron. Lett. 4 (2008) 0209−0212.

[51] P.F. Wang, Z.R. Hong, Z.Y. Xie, S.W. Tong, O.Y. Wong, C.S. Lee, N.B. Wong, L.S. Hung, S.T. Lee, Chem. Commun. (2003) 1664−1665.

[52] X.Q. Wei, Z.Y. Lu, P. Zou, M.G. Xie, Synth. Met. 137 (2003) 1149−1150.

[53] T.Z. Yu, W.M. Su, W.L. Li, Z.R. Hong, R.N. Hua, M.T. Li, B. Chu, B. Li, Z.Q. Zhang, Z.Z. Hu, Inorg. Chim. Acta 359 (2006) 2246−2251.

[54] T.Z. Yu, W.M. Su, W.L. Li, Z.R. Hong, R.N. Hua, B. Li, Thin Solid Films 515 (2007) 4080−4084.

[55] K.Y. Hwang, M.H. Lee, H. Jang, Y. Sung, J.S. Lee, S.H. Kim, Y. Do, Dalton Trans. (2008) 1818−1820.

[56] J.O. Huh, M.H. Lee, H. Jang, K.Y. Hwang, J.S. Lee, S.H. Kim, Y. Do, Inorg. Chem. 47 (2008) 6566−6568.

[57] L. Ying, C.-L. Ho, H. Wu, Y. Cao, W.-Y. Wong, Adv. Mater. 26 (2014) 2459−2473.

[58] F. Galbrecht, X.H. Yang, B.S. Nehls, D. Neher, T. Farrell, U. Scherf, Chem. Commun. (2005) 2378−2380.

[59] W.-L. Tong, L.-M. Lai, M.C.W. Chan, Dalton Trans. (2008) 1412−1414.

[60] S. Sun, W.-L. Tong, M.C.W. Chan, Macromol. Rapid Commun. 31 (2010) 1965−1969.

[61] O. Lavastre, I. Illitchev, G. Jegou, P.H. Dixneuf, J. Am. Chem. Soc. 124 (2002) 5278−5279.

[62] A.C.W. Leung, J.H. Chong, B.O. Patrick, M.J. MacLachlan, Macromolecules 36 (2003) 5051−5054.

[63] M. Nielsen, A.H. Thomsen, T.R. Jensen, H.J. Jakobsen, J. Skibsted, K.V. Gothelf, Eur. J. Org. Chem. 2 (2005) 342−347.

[64] C.C. Kwok, S.C. Yu, I.H.T. Sham, C.M. Che, Chem. Commun. (2004) 2758−2759.

[65] Q. Peng, M.Q. Xie, Y. Huang, Z.Y. Lu, Y. Cao, Macromol. Chem. Phys. 206 (2005) 2373−2380.

[66] X. de Hatten, N. Bell, N. Yufa, G. Christmann, J.R. Nitschke, J. Am. Chem. Soc. 133 (2011) 3158−3164,

[67] D. Asil, J.A. Foster, A. Patra, X. de Hatten, J. del Barrio, O.A. Scherman, J.R. Nitschke, R.H. Friend, Angew. Chem. Int. Ed. 53 (2014) 8388−8391.

[68] S.V. Eliseeva, J.-C.G. Bünzli, Chem. Soc. Rev. 39 (2010) 189−227.

[69] W.-K. Lo, W.-K. Wong, W.-Y. Wong, J.P. Guo, K.-T. Wong, Y.-K. Cheng, X.-P. Yang, R.A. Jones, Inorg. Chem. 45 (2006) 9315−9325.

[70] W.-K. Lo, W.-K. Wong, J.P. Guo, W.-Y. Wong, K.-F. Li, K.W. Cheah, Inorg. Chim. Acta 357 (2004) 4510−4521.

[71] W.-K. Wong, H.Z. Liang, W.-Y. Wong, Z.W. Cai, K.-F. Li, K.W. Cheah, New J. Chem. 26 (2002) 275−278.

[72] M. Andruh, Chem. Commun. (2007) 2565−2577.

[73] J. Long, L.M. Chamoreau, V. Marvaud, Dalton Trans. 39 (2010) 2188−2190.

[74] X.P. Yang, R.A. Jones, W.-K. Wong, V. Lynch, M.M. Oye, A.L. Holmes, Chem. Commun. (2006) 1836−1838.

[75] X.Q. Lu, W.Y. Bi, W.L. Chai, J.R. Song, J.X. Meng, W.-Y. Wong, W.-K. Wong, X.P. Yang, R.A. Jones, Polyhedron 28 (2009) 27−32.

[76] X.J. Zhu, W.-K. Wong, W.-Y. Wong, X.P. Yang, Eur. J. Inorg. Chem. (2011) 4651−4674.

[77] J. Zhao, F. Dang, B. Liu, Y. Wu, X. Yang, G. Zhou, Z. Wu, W.-Y. Wong, Dalton Trans. 46 (2017) 6098−6110.

[78] S.E. Shaheen, D.S. Ginley, G.E. Jabbour, MRS Bull. 30 (2005) 10−19.

[79] K.W.J. Barnham, M. Mazze, B. Clive, Nature 5 (2006) 161−164.

[80] C.-L. Ho, W.-Y. Wong, J. Photochem. Photobio. C: Photochem. Rev. 28 (2016) 138−158.

[81] C. Qin, W.-Y. Wong, L. Han, Chem. Asian J. 8 (2013) 1706−1719.

[82] S.V. Vasil'eva, I.A. Chepurnaya, S.A. Logvinov, P.V. Gaman'kov, A.M. Timonov, Russ. J. Electrochem. 39 (2003) 344−348.

[83] E.A. Smirnova, M.A. Besedina, M.P. Karushev, V.V. Vasil'ev, A.M. Timonov, Russ. J. Phys. Chem. A 90 (2016) 1088−1094.

[84] J. Kesters, P. Verstappen, M. Kelchtermans, L. Lutsen, D. Vanderzande, W. Maes, Adv. Energy Mater. 5 (2015) 1500218.

[85] M. Urbani, M. Grätzel, M.K. Nazeeruddin, T. Torres, Chem. Rev. 114 (2014) 12330−12396.

[86] S. Mathew, A. Yella, P. Gao, R. Humphry-Baker, B.F. Curchod, N. Ashari-Astani, I. Tavernelli, U. Rothlisberger, M.K. Nazeeruddin, M. Grätzel, Nat. Chem. 6 (2014) 242−247.

[87] Q. Tan, X. Zhang, L. Mao, G. Xin, S. Zhang, J. Mol. Struct. 1035 (2013) 400−406.

[88] A.W. Jeevadason, K.K. Murugavel, M.A. Neelakantan, Renew. Sustain. Energy

Rev. 36 (2014) 220−227.

[89] X. Zhang, C. Liao, J. Cao, L. Yang, Q. Li, J. Comp. Theor. Nanosci. 12 (2015) 2745−2750.

[90] Y. Wu, J.-C. Liu, J. Cao, R.-Z. Li, N.-Z. Jin, Res. Chem. Intermed. 41 (2015) 6833−6842.

[91] M. Nasr-Esfahani, M. Zendehdel, N.Y. Nia, B. Jafari, M.K. Babadi, RSC Adv. 4 (2014) 15961−15967.

[92] S.M. Yang, H.Z. Kou, H.J. Wang, K. Cheng, J.C. Wang, New J. Chem. 34 (2010) 313−317.

[93] Y.W. Dong, R.Q. Fan, P. Wang, L.G. Wei, X.M. Wang, H.J. Zhang, S. Gao, Y.L. Yang, Y.L. Wang, Dalton Trans. 44 (2015) 5306−5322.

[94] J.H. Yang, H.L. Yip, A.K.Y. Jen, Adv. Energy Mater. 3 (2013) 549−565.

[95] Q. Zhang, Y. Sun, W. Xu, D. Zhu, Adv. Mater. 26 (2014) 6829−6851.

[96] M. He, F. Qiu, Z.Q. Lin, Energy Environ. Sci. 6 (2013) 1352−1361.

[97] B.T. McGrail, A. Sehirlioglu, E. Pentzer, Angew. Chem. Int. Ed. 54 (2015) 1710−1723.

[98] N. Toshima, M. Imai, S. Ichikawa, J. Electron. Mater. 40 (2011) 898−902.

[99] K.F. Hsu, S. Loo, F. Guo, W. Chen, J.S. Dyck, C. Uher, T. Hogan, E.K. Polychroniadis, M.G. Kanatzidis, Science 303 (2004) 818−821.

[100] L.-D. Zhao, S.-H. Lo, Y. Zhang, H. Sun, G. Tan, C. Uher, C. Wolverton, V.P. Dravid, Nature 508 (2014) 373−377.

[101] Y. Sun, P. Sheng, C. Di, F. Jiao, W. Xu, D. Qiu, D. Zhu, Adv. Mater. 24 (2012) 932−937.

[102] M. Spiratos, G.I. Rusu, A. Airinei, A. Ciobanu, Die Angew. Makromol. Chem. 107 (1982) 33−42.

[103] J.T. Dsa, V.J. Rao, K.C. Patel, R.D. Patel, Die Angew. Makromol. Chem. 79 (1979) 133−145.

[104] B.J. Holliday, T.M. Swager, Chem. Commun. (2005) 23−36.

[105] B.J. Holliday, T.B. Stanford, T.M. Swager, Chem. Mater. 18 (2006) 5649−5651.

[106] M.T. Nguyen, B.J. Holliday, Chem. Commun. 51 (2015) 8610−8613.

[107] M.L. Mejia, G. Reeske, B.J. Holliday, Chem. Commun. 46 (2010) 5355−5357.

[108] W. Liu, W. Huang, C.-H. Chen, M. Pink, D. Lee, Chem. Mater. 24 (2012) 3650−3658.

[109] S. Suganya, F.P. Xavier, K.S. Nagaraja, Bull. Mater. Sci. 21 (1998) 403−407.

[110] A.V. Pardhi, A.D. Bansod, A.R. Yaul, A.S. Aswar, Russ. J. Coord. Chem. 36 (2010) 298−304.

[111] M. Winter, R. J. Brodd, Chem. Rev. 104 (2004) 4245−4270.

[112] T.B. Schon, B.T. McAllister, O.-F. Li, D.S. Seferos, Chem. Soc. Rev. 45 (2016) 6345−6404.

[113] P. Simon, Y. Gogotsi, Nat. Mater. 7 (2008) 845−854.

[114] G. Wang, L. Zhang, J. Zhang, Chem. Soc. Rev. 41 (2012) 797−828.

[115] J.-M. Tarascon, M. Armand, Nature 414 (2001) 359−367.

[116] F. Cheng, J. Liang, Z. Tao, J. Chen, Adv. Mater. 23 (2011) 1695−1715.

[117] B. Scrosati, J. Hassoun, Y.-K. Sun, Energy Environ. Sci. 4 (2011) 3287−3295.

[118] Y. Liang, Z. Tao, J. Chen, Adv. Energy Mater. 2 (2012) 742−769.

[119] K. Oyaizu, H. Nishide, Adv. Mater. 21 (2009) 2339−2344.

[120] T. Janoschka, M.D. Hager, U.S. Schubert, Adv. Mater. 24 (2012) 6397−6409.

[121] H. Nishide, K. Koshika, K. Oyaizu, Pure Appl. Chem. 81 (2009) 1961−1970.

[122] M. Lopez-Herraiz, E. Castillo-Martinez, J. Carretero-Gonzalez, J. Carrasco, T. Rojo, M. Armand, Energ. Environ. Sci. 8 (2015) 3233−3241.

[123] E. Castillo-Martinez, J. Carretero-Gonzalez, M. Armand, Angew. Chem. Int. Ed. 53 (2014) 5341−5345.

[124] Y.B. Sun, Y.H. Sun, Q.Y. Pan, G. Li, B. Han, D.L. Zeng, Y.F. Zhang, H.S. Cheng, Chem. Commun. 52 (2016) 3000−3002.

[125] X.W. Yang, X.D. Zhuang, Y.J. Huang, J.Z. Jiang, H. Tian, D.Q. Wu, F. Zhang, Y.Y. Mai, X.L. Feng, Polym. Chem. 6 (2015) 1088−1095.

[126] B. He, W.C. Li, A.H. Lu, J. Mater. Chem. A 3 (2015) 579−585.

[127] J.L. Segura, M.J. Mancheño, F. Zamora, Chem. Soc. Rev. 45 (2016) 5635−5671.

[128] T. Ren, Chem. Rev. 108 (2008) 4185−4207.

[129] H. Xu, J. Gao, D.L. Jiang, Nat. Chem. 7 (2015) 905−912.

[130] F. Franceschi, E. Solari, C. Floriani, M. Rosi, A. Chiesi-Villa, C. Rizzoli, Chem. Eur. J. 5 (1999) 708−721.

[131] C.-M. Che, S.-C. Chan, US Patent US2005/0233167 A1, (2005).

Captions for Figures

Fig. 1. Common types of metal Schiff base chromophores.

Fig. 2. UV-vis absorption spectra of Pt(II) Schiff base complexes (a) **25**–**29** and (b) **30**–**34** in CH_2Cl_2 (1.0×10^{-5} M) at room temperature.

Fig. 3. Emission spectra of Pt(II) Schiff base complexes (a) **25**–**29** and (b) **30**–**34** in CH_2Cl_2 (1.0×10^{-5} M) at room temperature **.**

Fig. 4. Representative EL spectra of the OLED fabricated with 8 wt% **31** at the driving voltage from 5 to 13 V.

Fig. 5. Performance of WOLED using a single emissive layer of **31** and FIrpic dopants: (a) EL spectrum; (b) power efficiency-luminance, luminance efficiency-luminance and external quantum efficiency-luminance curves.

Fig. 6. Synthesis of some 3d-4f bimetallic Schiff base complexes **88**.

Fig. 7. Representative examples of the formation of mixed-metal Schiff base complexes of various metal nuclearity **89**–**92**.

Fig. 8. Structure of poly-[M(salen)] polymers (M = Ni, Pd, Pt).

Fig. 9. A molecular battery system based on carbon-carbon bond formation and cleavage in titanium and vanadium Schiff base complexes. *Salphen$_2$* is a dinucleating, octadentate, octaanionic ligand.